

Theory of Saturated-Absorption Line Shapes*

Serge Haroche

*Laboratoire de l'Horloge Atomique du Centre National de la Recherche Scientifique,
91 Orsay, France*

and

*Laboratoire de Spectroscopie Hertzienne de l'Ecole Normale Supérieure,
24 rue Lhomond, Paris 5e, France†*

and

Francis Hartmann

*Laboratoire de l'Horloge Atomique du Centre National de la Recherche Scientifique,
91 Orsay, France*

(Received 30 March 1972)

A general theory of the saturated-absorption phenomenon in a two-level atomic system is developed, in which the phase relationships between the oscillating atomic dipoles as well as the population differences between energy levels are taken into account. The absorbing gaseous medium considered in this theory is subjected to irradiation by a quasi-running-wave composed of a strong pump field and a weak probe field propagating in opposite directions. Some new interesting results, not predicted by the so-called hole-burning or rate-equation model, are obtained. In particular, the probe-field-transmission peak line shape is found to be markedly different from what is expected according to the rate equations. For finite Doppler widths and a strong saturating pump field, absorption of the probe field can even change sign, and amplification of this field can actually occur. All these features are explained by a close inspection of the evolution of each atomic ensemble of given velocity. Detailed comparison with similar phenomena already observed in rf experiments is presented and permits us to clarify the new predicted effects.

INTRODUCTION

Resolution in optical spectroscopy of gases has long been limited by the Doppler effect, which gives to each line a relative width $\Delta\nu_d/\nu \approx 10^{-6}$. The recently appeared saturated-absorption technique¹ can lead to a substantial improvement in this respect. By making use of the nonlinear response characteristic of an atomic system to strong electromagnetic waves, one can essentially select for observation only those atoms which have a zero axial velocity. The absorption spectrum of the sample then consists in a Doppler-broadened line with a narrow dip of width $\Delta\nu_n$ appearing on its center. This dip, which is closely related to the Lamb dip appearing on the output of gas lasers as the cavity is tuned across the emission line, can be orders of magnitude narrower than the Doppler width $\Delta\nu_d$. The technique is already being used in spectroscopy² and for laser-frequency-stabilization purposes.³

Such a saturated-absorption dip (or transmission peak) appears when two counterrunning waves are allowed to propagate in the absorption cell. To account for the appearance of the peak, the so-called "hole-burning model" has been often used.^{4,5} For atoms with velocity \vec{v} , the two waves at frequency ω in the laboratory frame appear as having two different frequencies $\omega_+ = \omega - \vec{k} \cdot \vec{v}$ and $\omega_- = \omega + \vec{k} \cdot \vec{v}$, where \vec{k} is the wave vector ($k = \omega/c$). The hole-

burning (or rate-equations) model amounts to saying that one of the counterrunning waves saturates the class of atoms which have the right axial velocity. The transparency of the medium to the second wave, which is at a different frequency in the atomic frame, is not affected by the first except when the two frequencies happen to coincide in the atomic frame, that is when $\vec{k} \cdot \vec{v} = 0$ (atoms with zero axial velocity). The saturation of the atoms by the first wave then causes an increase in the transparency of the medium relative to the second wave.

Although it correctly predicts the appearance of a transmission peak, the above explanation remains qualitative, since it deals only with population changes and neglects the fact that the atomic dipoles which absorb one wave are coherently driven by the other. In particular, it is well known that irradiation of an atomic system by a strong electromagnetic wave not only affects the populations of the various states but can also modify appreciably the atomic eigenstates, occasioning level shifts⁶ or dynamic Stark-splitting effects⁷ in the atomic system. Furthermore, when two waves simultaneously couple with the atomic system, nonlinear effects such as Raman or multiple-photon processes may also occur. All these phenomena, which are disregarded in the "hole-burning" model, may become rather important if at least one of the counterrunning waves has a large intensity and have, thus, to be accounted for in an accurate theory of saturated absorption.

A case of particular interest for the study of these effects is the quasi-running-wave situation corresponding to the irradiation of the medium by a strong saturating field (the so-called pump field) and a weak-counterrunning probe field tuned at the same frequency which explores the medium saturated by the first one. Such a situation is in fact practically realized in many saturated-absorption experiments⁵ and has already been theoretically considered in a recent publication⁸ where the inadequacies of the hole-burning model have been pointed out.

The purpose of this paper is to develop a complete theory of saturated absorption in the quasi-running-wave situation, which stands as an independent treatment of the subject matter.⁹ This theory generalizes the results obtained in the above-mentioned publication and leads to the prediction of some new original effects.

As is done in Ref. 8 and in various other publications dealing with gas-lasers theories,¹⁰⁻¹³ the gaseous active medium under consideration in this paper is an ensemble of two-level atoms of molecules described by its density matrix, and the evolution of the atomic dipoles, as well as that of the levels populations, is explicitly considered. The electromagnetic (em) waves to which the atomic system is coupled are described classically. To account for the quasi-running-wave situation of interest here, the effect of the strong field on the medium is dealt with exactly, whatever its intensity, while the interaction with the probe is described in a perturbative way. However, instead of limiting the perturbation treatment to first order in probe amplitude as is done in Ref. 8, we present a formalism which allows an iterative calculation of the atomic response to any desired order in probe strength, and perform explicitly the calculation up to second order, which yields the determination of several quantities of physical interest.

The probe-absorption line shape is obtained as a result of the calculation carried up to first order. The line shape is found to be markedly different from what is predicted by rate equations. While the hole-burning model leads to a complete saturation of the probe absorption for large pump-field intensities, it is shown as in Ref. 8, that in the case of a large Doppler width the medium can in fact never become completely transparent to the probe wave.

In addition to this effect, some new results not discussed before are also put into evidence. When the Doppler width is only a few times the homogeneous width and the pump field is strong enough, we show that the absorption may on the contrary be fully saturated and that the probe-absorption coefficient can even change sign. The medium then exhibits amplification on the return wave,

which may seem a rather strange and peculiar effect since there is no population inversion in the two-level atomic system.

In fact we will show that the probe amplification is essentially obtained in this case at the expense of the pump field which experiences a further attenuation when the probe is turned on. The relevant energy balance is easily obtained from our perturbative calculation carried up to second order. This calculation also allows the determination of the population difference saturated by the two waves. A "fine structure" in the center of the population difference versus velocity curve is predicted, which provides an interesting link with similar effects already discussed in high-intensity laser theories.¹¹⁻¹³

All these phenomena are explained by a close inspection of the evolution of each atomic ensemble of given axial velocity v . Level-splitting effects and nonlinear processes occurring in the atomic rest frame are thoroughly described in order to stress the incompleteness of the hole-burning model. Detailed comparison with similar well-known effects already observed in rf experiments are presented and permit us to clarify the new predicted phenomena.

The outline of the paper will be as follows: We will first derive the general equations of motion of the atomic system (Sec. I) and study the general form of their solution (Sec. II) which can be expanded in Fourier series along the spatial harmonics nk of the wave vector. In Sec. III, we will relate some of the Fourier coefficients thus obtained to the physical quantities of interest for our saturated-absorption problem and will then explicitly calculate these coefficients in Sec. IV. We will thus be in a position to study in detail the absorption of the probe field for each atomic ensemble of given velocity (Sec. V). Then, after integration over the velocity distribution, we will study the saturated-absorption line shape itself (Sec. VI). We will consider in Sec. VII the reaction of the probe field on the pump field and atomic medium. In an Appendix, we will finally extend the theory to the case of a probe field whose frequency is different from that of the pump field.

I. EQUATIONS OF MOTION OF THE ATOMIC SYSTEM

A. Description of Atomic System

We consider an ensemble of atoms (or molecules) with two energy levels a and b separated by an energy interval $E_a - E_b = \hbar\omega_0$ (Fig. 1) and assume that radiative transitions are possible between these two levels (we will be specifically interested in the response of the atoms to em fields quasiresonant with the atomic frequency ω_0 and can then disregard all other energy states of the system). Such an

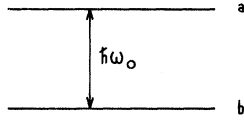


FIG. 1. Two energy levels a and b between which saturated absorption takes place. The levels have a resonance transition frequency ω_0 and are given phenomenological decay constants γ_a and γ_b , whereas the dipole moment between them is damped at a rate γ_{ab} . The excitation rates of these states are described by the quantities λ_a and λ_b defined in Eq. (4).

ensemble is conveniently described by a 2×2 density matrix ρ in which the diagonal elements account for the populations of the two levels, and the nondiagonal element is proportional to the atomic dipole moment. The em fields of interest to us will be those of plane waves propagating along the z direction. The corresponding perturbation "seen" by a given atom then depends on z and t but also, due to the Doppler effect, on its axial velocity v .

It is thus convenient to define first a density matrix $\rho(z, t, v)$ describing the ensemble-averaged properties of atoms passing at point z , at time t , with axial velocity v . Once the evolution of $\rho(z, t, v)$ is known, the value of any observable Q attached to the atoms in the volume element of phase space under consideration can be calculated by the usual formula

$$\langle Q(z, t, v) \rangle = \text{Tr}[\rho(z, t, v)Q], \quad (1)$$

where, if necessary, values of Q averaged upon velocity and position can be obtained from

$$\langle Q(z, t) \rangle = \int_{-\infty}^{+\infty} \langle Q(z, t, v) \rangle dv, \quad (2)$$

$$\langle Q(t) \rangle = \int_0^L \langle Q(z, t) \rangle dz, \quad (3)$$

where L is the length of the absorbing cell.

The atoms we are considering are subjected to relaxation processes which can be phenomenologically accounted for by damping constants. We will suppose that levels a and b decay with rate constants γ_a and γ_b , whereas the atomic dipole moment decays at a rate γ_{ab} . Moreover, we will assume that some excitation mechanism populates levels a and b at rates λ_a and λ_b per unit time and unit volume element $dz dv$ of phase space. The exact value of all these constants depends of course on the nature of the processes involved (spontaneous emission, atomic collisions...). For sake of simplicity, we will consider here that they do not depend on z and t . We will also consider γ_a , γ_b , and γ_{ab} as velocity independent; on the other hand, the excitation rates λ_a and λ_b will be assumed to be of the form

$$\lambda_i(v) = \Lambda_i W(v) \quad (i = a, b), \quad (4)$$

where

$$W(v) = (\pi^{1/2} v_m)^{-1} e^{-v^2/v_m^2} \quad (5)$$

is the normalized velocity distribution with a most probable velocity $v_m = (2k_B T/M)^{1/2}$ at temperature T .

The variation with time of the density-matrix elements under the action of excitation and relaxation processes is then given by

$$\begin{aligned} \left(\frac{d\rho_{aa}}{dt}(z, t, v) \right)_{e+r} &= \lambda_a(v) - \gamma_a \rho_{aa}(z, t, v), \\ \left(\frac{d\rho_{bb}}{dt}(z, t, v) \right)_{e+r} &= \lambda_b(v) - \gamma_b \rho_{bb}(z, t, v), \\ \left(\frac{d\rho_{ab}}{dt}(z, t, v) \right)_{e+r} &= -\gamma_{ab} \rho_{ab}(z, t, v). \end{aligned} \quad (6)$$

Let us emphasize that with our assumptions the relaxation processes affect only the internal state of the atoms without changing their velocity; the Maxwellian velocity distribution at thermal equilibrium is ensured by the form chosen for the excitation constants λ_i . The population difference reached under the only action of excitation and relaxation process [$d\rho/dt = 0$ in Eq. (6)] is indeed given by

$$\begin{aligned} [\rho_{aa}(z, t, v) - \rho_{bb}(z, t, v)]_0 &= (\Lambda_a/\gamma_a - \Lambda_b/\gamma_b)W(v) \\ &= N_0 W(v), \end{aligned} \quad (7)$$

where

$$N_0 = \Lambda_a/\gamma_a - \Lambda_b/\gamma_b \quad (8)$$

is the total population difference at equilibrium per unit length of the cell.

B. Evolution in Presence of Electromagnetic Fields

We now assume that the system described above is subjected to two electromagnetic waves of the same angular frequency $\omega = ck$ propagating in opposite directions along the z axis and polarized along the x direction. We will write them in the form

$$\begin{aligned} E_+ &= \epsilon_+ \cos(\omega t - kz), \\ E_- &= \epsilon_- \cos(\omega t + kz). \end{aligned} \quad (9)$$

One of the fields (ϵ_+) may be strong enough to saturate the medium, whereas the other (ϵ_-) will always be considered as a weak perturbation. (The latter field may for instance be created by a reflection of the strong field on a weakly reflecting mirror perpendicular to the z axis.) Let us notice that the assumed expressions (9) for the em fields imply that their amplitudes do not depend on the penetration depth z (weak-absorption limit).

The Hamiltonian of the two-level system subjected to this perturbation can be written

$$\mathcal{H} = \mathcal{H}_0 - PE_+ - PE_-, \quad (10)$$

where \mathcal{H}_0 is the free-atom Hamiltonian

$$\mathcal{H}_0 = \frac{\hbar\omega_0}{2} \begin{pmatrix} 1 & 0 \\ 0 & -1 \end{pmatrix}, \quad (11)$$

and P is the x component of the atomic dipole moment. This operator has only off-diagonal matrix elements which can always be written as

$$\langle a | P | b \rangle = \langle b | P | a \rangle = \mathcal{P}, \quad (12)$$

where \mathcal{P} is a real number. We then have

$$\mathcal{H}(z, t) = \frac{\hbar\omega_0}{2} \begin{pmatrix} 1 & 0 \\ 0 & -1 \end{pmatrix} - \mathcal{P}\epsilon_+ \cos(\omega t - kz) \begin{pmatrix} 0 & 1 \\ 1 & 0 \end{pmatrix} - \mathcal{P}\epsilon_- \cos(\omega t + kz) \begin{pmatrix} 0 & 1 \\ 1 & 0 \end{pmatrix}. \quad (13)$$

We will restrict ourselves to the case where ω is very close to the atomic frequency ω_0 , which enables us to make the rotating-wave approximation. Then we have

$$\mathcal{H}(z, t) \approx \frac{\hbar\omega_0}{2} \begin{pmatrix} 1 & 0 \\ 0 & -1 \end{pmatrix} - \frac{\mathcal{P}\epsilon_+}{2} \begin{pmatrix} 0 & e^{-i(\omega t - kz)} \\ e^{i(\omega t - kz)} & 0 \end{pmatrix} - \frac{\mathcal{P}\epsilon_-}{2} \begin{pmatrix} 0 & e^{-i(\omega t + kz)} \\ e^{i(\omega t + kz)} & 0 \end{pmatrix}. \quad (14)$$

The total time variation of the density matrix is obtained by adding the contributions due to excitation, relaxation, and the action of the em fields:

$$\frac{d\rho}{dt}(z, t, v) = \left(\frac{d\rho(z, t, v)}{dt} \right)_{e++} - \frac{i}{\hbar} [\mathcal{H}(z, t), \rho(z, t, v)]. \quad (15)$$

In this equation the operator d/dt is a total time derivative along the path of the atoms moving with velocity v , so that one has $d/dt = \partial/\partial t + v\partial/\partial z$. We then obtain for the evolution of the density matrix $\rho(z, t, v)$ the so-called "hydrodynamic equation" already used by various authors^{8,13,14}

$$\left(\frac{\partial}{\partial t} + v \frac{\partial}{\partial z} \right) \rho(z, t, v) = \left(\frac{d}{dt} \rho(z, t, v) \right)_{e++} - \frac{i}{\hbar} [\mathcal{H}(z, t), \rho(z, t, v)], \quad (16)$$

which gives for the different matrix elements

$$\left(\frac{\partial}{\partial t} + v \frac{\partial}{\partial z} \right) \rho_{aa} = \lambda_a - \gamma_a \rho_{aa} - i \frac{\mathcal{P}\epsilon_+}{2\hbar} (\rho_{ab} e^{i(\omega t - kz)} - \rho_{ba} e^{-i(\omega t - kz)}) - i \frac{\mathcal{P}\epsilon_-}{2\hbar} (\rho_{ab} e^{i(\omega t + kz)} - \rho_{ba} e^{-i(\omega t + kz)}), \quad (17a)$$

$$\left(\frac{\partial}{\partial t} + v \frac{\partial}{\partial z} \right) \rho_{bb} = \lambda_b - \gamma_b \rho_{bb} + i \frac{\mathcal{P}\epsilon_+}{2\hbar} (\rho_{ab} e^{i(\omega t - kz)} - \rho_{ba} e^{-i(\omega t - kz)}) + i \frac{\mathcal{P}\epsilon_-}{2\hbar} (\rho_{ab} e^{i(\omega t + kz)} - \rho_{ba} e^{-i(\omega t + kz)}), \quad (17b)$$

$$\left(\frac{\partial}{\partial t} + v \frac{\partial}{\partial z} \right) \rho_{ab} = -(\gamma_{ab} + i\omega_0) \rho_{ab} - i \frac{\mathcal{P}\epsilon_+}{2\hbar} (\rho_{aa} - \rho_{bb}) e^{-i(\omega t - kz)} - i \frac{\mathcal{P}\epsilon_-}{2\hbar} (\rho_{aa} - \rho_{bb}) e^{-i(\omega t + kz)}. \quad (17c)$$

II. GENERAL FORM OF SOLUTION

We want to obtain the steady-state solution of Eq. (17) in the quasi-running-wave situation corresponding to a strong saturating field ϵ_+ and a weak probe field ϵ_- . A natural procedure, already used for the study of nonlinear susceptibilities,¹⁵ consists in first looking for a solution in the presence of only the strong field ϵ_+ and then considering the action of the weak field ϵ_- as a perturbation which will slightly modify the solution thus obtained. We will, therefore, first recall the well-known results concerning the response of an atomic system to a running wave.

A. Solution in Running-Wave Case

In the case when only ϵ_+ is present, the system (17) can be solved exactly. Looking for a steady-state solution of the form

$$\rho_{aa}(z, t, v) = \alpha_{a0}^{(0)}(v),$$

$$\rho_{bb}(z, t, v) = \alpha_{b0}^{(0)}(v),$$

$$\rho_{ab}(z, t, v) = \beta_0^{(0)}(v) e^{-i(\omega t - kz)}, \quad (18)$$

one obtains, by inserting these expressions into Eq. (17), a system of algebraic equations which can be solved to give

$$\beta_0^{(0)}(v, \omega, I) = -i \frac{\mathcal{P}\epsilon_+}{2\hbar} N_0 W(v) \times \frac{\gamma_{ab} - i(\omega_0 - \omega + kv)}{\gamma_{ab}^2 + (\omega_0 - \omega + kv)^2 + I^2 \gamma_{ab}^2}, \quad (19a)$$

$$N^{(0)}(v, \omega, I) \equiv \alpha_{a0}^{(0)}(v, \omega, I) - \alpha_{b0}^{(0)}(v, \omega, I) = N_0 W(v) \left(1 - \frac{I^2 \gamma_{ab}^2}{\gamma_{ab}^2 + (\omega_0 - \omega + kv)^2 + I^2 \gamma_{ab}^2} \right). \quad (19b)$$

In these equations, we have introduced the quantity

$$I^2 = \mathcal{P}^2 \epsilon_+^2 / \hbar^2 \gamma \gamma_{ab}, \quad (20)$$

which is a dimensionless number proportional to the intensity of the traveling wave ϵ_+ . In this expression, a new decay rate γ is defined by

$$2/\gamma = 1/\gamma_a + 1/\gamma_b. \quad (21)$$

Formulas (19) have a simple and well-known interpretation. Equation (19a) shows that the dipole moment of atoms with velocity v exhibits a resonant variation when the frequency ω of the traveling wave obeys the relation

$$\omega - kv = \omega_0, \quad (22)$$

which corresponds to the matching between the atomic frequency ω_0 and the Doppler-shifted frequency $\omega_* = \omega - kv$ of the traveling wave in the atom rest frame. Equation (19b) shows that the population difference as a function of velocity follows the Maxwellian distribution $W(v)$, with an additional minimum when the resonance condition (22) is fulfilled. The minimum corresponds to the "hole" burnt into the population distribution by the traveling wave. The resonant variation of expressions (19a) and (19b) has a width γ_{ab} at low-field amplitudes and exhibits a saturation broadening when the intensity I^2 of the traveling wave is increased.

Let us emphasize that the solutions (19) are exact ones (within the validity of the rotating-wave approximation) and hold for an arbitrarily large value of the saturation parameter I^2 . Such an exact solution can be derived for the special case of a pure traveling wave because each class of atoms with a given velocity v "sees" a single frequency $\omega_* = \omega - kv$ in its rest frame; one is thus led for this class of atoms to solve the problem of a two-level system subjected to a quasiresonant monochromatic excitation, which is formally equivalent to the well-known solvable problem of the magnetic resonance in a spin one-half system.¹⁶

If one now takes into account the weak probe field ϵ_- running in the opposite direction, it is clear that each class of atoms will experience two electromagnetic perturbations whose frequencies $\omega_* = \omega - kv$ and $\omega_- = \omega + kv$ will generally be different in the atom rest frame. This corresponds to a much more intricate problem which was already studied in the case of a standing wave excitation ($\epsilon_- = \epsilon_+$)¹⁰⁻¹³ whereas we intend here to solve it in the quasi-running-wave situation ($\epsilon_- \ll \epsilon_+$).

B. Perturbation Expansion of General Solution

In order to calculate the perturbation caused by the weak ϵ_- field to the "zero-order solution" obtained above, we are led to expand the density matrix $\rho(z, t, v)$ in increasing powers of ϵ_- :

$$\rho(z, t, v) = \rho^{(0)}(z, t, v) + \rho^{(1)}(z, t, v)\epsilon_- + \dots + \rho^{(p)}(z, t, v)\epsilon_-^p + \dots \quad (23)$$

If we insert the formal development (23) into the system (17) and identify in both sides of the equations terms containing the same powers of ϵ_- , we will get a set of recurrent linear differential equations coupling $\rho^{(1)}$ to $\rho^{(0)}$, $\rho^{(2)}$ to $\rho^{(1)}$, and generally $\rho^{(p)}$ to $\rho^{(p-1)}$. From the knowledge of $\rho^{(0)}$ determined above, we are thus able to calculate the solution to any desired order.¹⁵

Before performing this iteration we can make some remarks upon the general form of the solution which will considerably simplify the calculations. Let us first notice that all off-diagonal components $\rho_{ab}^{(p)}$ will have a time variation proportional to $e^{-i\omega t}$, whereas all diagonal components $\rho_{aa}^{(p)}$ and $\rho_{bb}^{(p)}$ will be time independent. This result holds for $p=0$ as is easily seen in Eq. (19). It can be proved to any order p by direct substitution in Eq. (17) of a solution of the form

$$\rho_{ab}(z, t, v) = \rho_{ab}(z, v) e^{-i\omega t},$$

$$\rho_{jj}(z, t, v) = \rho_{jj}(z, v) \quad (j = a, b),$$

which gives time-independent equations for $\rho_{ab}(z, v)$ and $\rho_{jj}(z, v)$. This simple time dependence results from the fact that we have neglected, by making the rotating-wave approximation, all off-resonant components of the em field which would have generated higher-order time-varying harmonics in the atomic density matrix.

Another important property of the steady-state solution of Eq. (17) follows from the iterative relationship between diagonal and off-diagonal matrix elements of ρ . The population difference $\rho_{aa} - \rho_{bb}$, which is spatially uniform to zero order, couples in Eq. (17c) with the em field to give terms in ρ_{ab} varying in space as $e^{\pm ikz}$; these react back through Eq. (17a) and (17b) on ρ_{aa} and ρ_{bb} to create components varying as $e^{\pm 2ikz}$ and so on. As a result the density matrix is spatially modulated at all harmonics qk of the wave vector, with only odd harmonics appearing in the expansion of ρ_{ab} and only even harmonics in the expansion of ρ_{aa} and ρ_{bb} . As was already noticed¹³ these spatial modulations correspond in the atom rest frame to temporal modulations at frequencies qkv ; these modulations are induced through the coupling of the atoms with the two waves running in opposite directions which are "seen" as monochromatic perturbations with frequencies $\omega_* = \omega - kv$ and $\omega_- = \omega + kv$.

With all these properties in mind, we may now expand the general term $\rho^{(p)}(z, t, v)$ of the development (23) in the following form:

$$\rho_{aa}^{(p)} = \sum_n \alpha_{an}^{(p)} e^{2in kz}, \quad (24a)$$

$$\rho_{bb}^{(p)} = \sum_n \alpha_{bn}^{(p)} e^{2in kz}, \quad (24b)$$

$$\rho_{ab}^{(p)} = \sum_n \beta_n^{(p)} e^{2in kz} e^{-i(\omega t - kz)}, \quad (24c)$$

$$\rho_{ba}^{(p)} = \sum_n \beta_n^{(p)} e^{2inkz} e^{i(\omega t - kz)}. \quad (24d)$$

The Fourier coefficients $\alpha_{an}^{(p)}$, $\alpha_{bn}^{(p)}$, $\beta_n^{(p)}$, and $\beta_n^{\prime(p)}$ thus defined are functions of v , ω , and I which obey the following relations corresponding to the Hermitian character of ρ :

$$\alpha_{jn}^{(p)*} = \alpha_{j,-n}^{(p)} \quad (j = a, b), \quad (25a)$$

$$\beta_n^{(p)*} = \beta_{-n}^{\prime(p)}. \quad (25b)$$

Inserting (24) and (23) in (17) and taking account of (25), we finally get a set of linear algebraic relations which allow the recurrent calculation of all Fourier coefficients:

$$(\gamma_a + 2inkv)\alpha_{an}^{(p)} = -i \frac{\mathcal{P}\epsilon_{\pm}}{2\hbar} (\beta_n^{(p)} - \beta_{-n}^{(p)*}) - i \frac{\mathcal{P}}{2\hbar} (\beta_{n-1}^{(p-1)} - \beta_{-n-1}^{(p-1)*}), \quad (26a)$$

$$(\gamma_b + 2inkv)\alpha_{bn}^{(p)} = i \frac{\mathcal{P}\epsilon_{\pm}}{2\hbar} (\beta_n^{(p)} - \beta_{-n}^{(p)*}) + i \frac{\mathcal{P}}{2\hbar} (\beta_{n-1}^{(p-1)} - \beta_{-n-1}^{(p-1)*}), \quad (26b)$$

$$[\gamma_{ab} + i(\omega_0 - \omega) + i(2n+1)kv]\beta_n^{(p)} = -i \frac{\mathcal{P}\epsilon_{\pm}}{2\hbar} (\alpha_{an}^{(p)} - \alpha_{bn}^{(p)}) - i \frac{\mathcal{P}}{2\hbar} (\alpha_{an+1}^{(p-1)} - \alpha_{bn+1}^{(p-1)}). \quad (26c)$$

A direct inspection of these equations valid for $p > 0$ easily shows that the coefficients corresponding to given orders p and $\pm n$ are related only to those of orders $p-1$ and $\pm n \pm 1$. As the zero-order solution corresponds to $p=0$ and $n=0$, we see that the only nonzero Fourier coefficients are those with p and n of the same parity and $|n| \leq p$.

C. Connection with Previous Gas-Lasers Theories

We must emphasize that Eqs. (26) allow an exact and explicit calculation of the atomic response to any desired order in the weak-field amplitude ϵ_{\pm} . As we will see later on some examples, this calculation consists in solving, to a given order, a closed set of coupled linear algebraic equations. We also notice that the solution is obtained as a perturbation expansion in ϵ_{\pm} , but that the effects of the strong wave ϵ_{\pm} are taken into account exactly, whatever its amplitude (or intensity I^2). This follows from the choice of the zero-order solution $\rho^{(0)}(z, t, v)$, in which the action of ϵ_{\pm} has been exactly dealt with. In this sense the treatment of the present paper differs by some important respects from those given in previous studies dealing with the Doppler effect in the presence of counter-running waves. In the first theory of gas lasers,¹⁰ the relevant em field was a standing wave ($\epsilon_{+} = \epsilon_{-}$), and the atomic response was developed in increasing powers of the common amplitude of both counter-running waves. As a con-

sequence of this perturbation treatment, valid results were obtained only for moderate field intensities. On the other hand, more recent papers on the theory of high-intensity gas lasers¹¹⁻¹³ give expressions for the response of the atomic medium which are valid for any amplitude of both counter-running waves. These expressions take the form of a Fourier expansion along the various spatial harmonics nk analogous to the one derived in this paper. However, the important difference is that the coefficients of these Fourier expansions are not developed in increasing powers of one of the em waves, since both fields are of the same amplitude. As a result, the Fourier coefficients defined in these papers cannot be put in a closed explicit form and are calculated from the resolution of an infinite set of coupled equations, so that (except in special cases^{13,17}) only solutions in terms of continued fractions can be obtained for them. Our approach thus appears as intermediate between those quoted above, being a semiperturbative treatment dealing exactly with the strong wave and perturbatively with the weak one. This leads, as we will see later on, to simpler calculations than those developed in high-intensity lasers theories. Our treatment nevertheless allows the prediction of very important saturation effects induced by the pump field, which is not the case for the theory presented in the first Lamb paper.¹⁰ On the other hand, the situation $\epsilon_{+} \gg \epsilon_{-}$ is, of course, only realizable outside the laser cavity itself.

III. PHYSICAL MEANING OF FOURIER COEFFICIENTS

Before giving the explicit form of the various Fourier coefficients which are solutions of Eq. (26) it is interesting to relate them to the different observables of the atomic medium. We will thus give a physical significance to some of these coefficients, enabling us to limit the calculation to the only terms of interest.

A. Atomic Polarization and Power Exchanged with Electromagnetic Fields

The polarization corresponding to the ensemble of atoms characterized by (z, t, v) is readily obtained from Eqs. (1) and (24):

$$P(z, t, v) = \mathcal{P} e^{-i(\omega t - kz)} (\beta_0^{(0)} + \sum_{p>0} \sum_n \epsilon_{\pm}^p \beta_n^{(p)} e^{2inkz}) + \text{c. c.}, \quad (27)$$

the prime on the summation over n meaning that it is restricted to $|n| \leq p$ with n and p of the same parity. It is useful to introduce the components P_{+} and P_{-} of the polarization having, respectively, the same spatio-temporal dependence as the pump and probe fields, E_{+} and E_{-} . One has

$$P_{\pm}(z, t, v) = \mathcal{P} e^{-i(\omega t - kz)} (\beta_0^{(0)} + \sum_{p \text{ even} > 0} \epsilon_{\pm}^p \beta_0^{(p)}) + \text{c. c.}, \quad (28a)$$

$$P_{\pm}(z, t, v) = \mathcal{P} e^{-i(\omega t + kz)} \left(\sum_{\rho \text{ odd} > 0} \epsilon_{\pm}^{\rho} \beta_{\pm 1}^{(\rho)} \right) + \text{c. c.} \quad (28b)$$

The linear and nonlinear susceptibilities relative to ϵ_{\pm} are clearly apparent in these equations. These susceptibilities are linked to the absorption and dispersion properties of the medium. We want here to calculate the energy transfer between the atomic medium and the two fields. If we call $G_{+}(v, \omega, I)$ and $G_{-}(v, \omega, I)$ the power per unit length and per unit velocity interval gained by the atoms with velocity v from the strong and weak field, respectively, we have

$$G_{\pm}(v, \omega, I) = \left\langle E_{\pm}(z, t) \frac{d}{dt} P_{\pm}(z, t, v) \right\rangle, \quad (29)$$

where $\langle \rangle$ indicates a time average (in which process the z dependence also disappears). From (28) and (29), one finds

$$G_{+}(v, \omega, I) = \omega \mathcal{P} \epsilon_{+} \text{Im}(\beta_0^{(0)} + \sum_{\rho \text{ even} > 0} \epsilon_{\pm}^{\rho} \beta_0^{(\rho)}), \quad (30a)$$

$$G_{-}(v, \omega, I) = \omega \mathcal{P} \epsilon_{-} \text{Im} \left(\sum_{\rho \text{ odd} > 0} \epsilon_{\pm}^{\rho} \beta_{-1}^{(\rho)} \right). \quad (30b)$$

We see that the power absorbed from the probe field to lowest order is given by the simple formula

$$G_{-}^{(1)}(v, \omega, I) = \omega \mathcal{P} \epsilon_{-}^2 \text{Im} \beta_{-1}^{(1)}. \quad (31)$$

On the other hand, the power absorbed from the strong saturating field in the absence of the weak probe field is given by

$$G_{+}^{(0)}(v, \omega, I) = \omega \mathcal{P} \epsilon_{+} \text{Im} \beta_0^{(0)}. \quad (32)$$

The presence of the weak field brings in a correction term

$$G_{+}^{(2)}(v, \omega, I) = \omega \mathcal{P} \epsilon_{+} \epsilon_{\pm}^2 \text{Im} \beta_0^{(2)}. \quad (33)$$

The total power absorbed in each case is finally obtained by integration of $G(v, \omega, I)$ over all velocities

$$G_{\pm}(\omega, I) = \int_{-\infty}^{+\infty} G_{\pm}(v, \omega, I) dv. \quad (34)$$

B. Population Difference Induced in Atoms System by Electromagnetic Fields

The spatially modulated population difference between states a and b for atoms at point z with velocity v is readily obtained from Eq. (24):

$$N(z, v, \omega, I) = \alpha_{a0}^{(0)} - \alpha_{b0}^{(0)} + \sum_{\rho > 0} \sum_n \epsilon_{\pm}^{\rho} (\alpha_{an}^{(\rho)} - \alpha_{bn}^{(\rho)}) e^{2in kz}, \quad (35)$$

where the prime on the summation over n has the same significance as before. The averaged population difference per unit length and unit velocity interval is thus

$$N(v, \omega, I) = \alpha_{a0}^{(0)} - \alpha_{b0}^{(0)} + \sum_{\rho \text{ even} > 0} \epsilon_{\pm}^{\rho} (\alpha_{a0}^{(\rho)} - \alpha_{b0}^{(\rho)}). \quad (36)$$

In this expression, $\alpha_{a0}^{(0)} - \alpha_{b0}^{(0)} = N^{(0)}(v, \omega, I)$ is the population difference saturated by the strong field, but in the absence of the weak field, given by Eq. (19b). This population difference is modified when the weak field is added, the lowest-order correction being

$$N^{(2)}(v, \omega, I) = \epsilon_{\pm}^2 (\alpha_{a0}^{(2)} - \alpha_{b0}^{(2)}). \quad (37)$$

Here again, the total population difference per unit length is obtained by integration over velocity.

It results from the above study that the Fourier coefficients of physical interest are, up to second order in ϵ_{\pm} : $\beta_{-1}^{(1)}$, $\beta_0^{(2)}$, and $\alpha_{a0}^{(2)} - \alpha_{b0}^{(2)}$. We will calculate them explicitly in Sec. IV.

IV. EXPLICIT CALCULATION OF SOLUTION UP TO SECOND ORDER

A. First-Order Solution: Linear Response to Weak Field

The linear response of the system to the probe field ϵ_{\pm} is obtained by solving Eqs. (26) corresponding to $p = 1$, $n = \pm 1$. Owing to the Hermitian character of ρ [see Eq. (25)], this set reduces to the following four linear equations for the coefficients $\alpha_{a1}^{(1)}$, $\alpha_{b1}^{(1)}$, $\beta_1^{(1)}$, and $\beta_{-1}^{(1)}$:

$$(\gamma_a + 2ikv) \alpha_{a1}^{(1)} + i \frac{\mathcal{P} \epsilon_{\pm}}{2\hbar} (\beta_1^{(1)} - \beta_{-1}^{(1)*}) = -i \frac{\mathcal{P}}{2\hbar} \beta_0^{(0)}, \quad (38a)$$

$$(\gamma_b + 2ikv) \alpha_{b1}^{(1)} - i \frac{\mathcal{P} \epsilon_{\pm}}{2\hbar} (\beta_1^{(1)} - \beta_{-1}^{(1)*}) = \frac{i\mathcal{P}}{2\hbar} \beta_0^{(0)}, \quad (38b)$$

$$[\gamma_{ab} + i(\omega_0 - \omega + 3kv)] \beta_1^{(1)} + i \frac{\mathcal{P} \epsilon_{\pm}}{2\hbar} (\alpha_{a1}^{(1)} - \alpha_{b1}^{(1)}) = 0, \quad (38c)$$

$$[\gamma_{ab} + i(\omega_0 - \omega - kv)] \beta_{-1}^{(1)} + i \frac{\mathcal{P} \epsilon_{\pm}}{2\hbar} (\alpha_{a1}^{(1)*} - \alpha_{b1}^{(1)*}) = -\frac{i\mathcal{P}}{2\hbar} (\alpha_{a0}^{(0)} - \alpha_{b0}^{(0)}). \quad (38d)$$

In the right-hand side of these equations appears the zero-order solution $\beta_0^{(0)}$ and $\alpha_{a0}^{(0)} - \alpha_{b0}^{(0)}$ given by Eqs. (19a) and (19b). The resolution of this system, straightforward but tedious, gives the following result for the susceptibility $\beta_{-1}^{(1)}$:

$$\beta_{-1}^{(1)}(v, \omega, I) = -i \frac{\mathcal{P}}{2\hbar \gamma_{ab}} (\alpha_{a0}^{(0)} - \alpha_{b0}^{(0)}) \frac{\gamma_{ab}}{\gamma_{ab}^2 + (\omega_0 - \omega - kv)^2} [\gamma_{ab} - i(\omega_0 - \omega - kv) - I^2 \gamma_{ab} B(v, \omega, I)], \quad (39)$$

where we have introduced the dimensionless quantity:

$$B(v, \omega, I) = \frac{[\gamma_{ab} - i(\omega_0 - \omega - kv)] \{ [\gamma_{ab} - i(\omega_0 - \omega + kv)]^{-1} + [\gamma_{ab} + i(\omega_0 - \omega - kv)]^{-1} \}}{2f(v) + I^2 \gamma_{ab} \{ [\gamma_{ab} - i(\omega_0 - \omega + 3kv)]^{-1} + [\gamma_{ab} + i(\omega_0 - \omega - kv)]^{-1} \}}, \quad (40)$$

with

$$f(v) = \frac{2}{\gamma} \frac{1}{(\gamma_a - 2ikv)^{-1} + (\gamma_b - 2ikv)^{-1}} \quad (41)$$

The other Fourier coefficients can readily be determined from $\beta_{-1}^{(1)}$. The quantity $\alpha_{a1}^{(1)} - \alpha_{b1}^{(1)}$, which will be of interest in the second-order calculation, is thus given by

$$\alpha_{a1}^{(1)} - \alpha_{b1}^{(1)} = -\frac{\alpha_{a0}^{(0)} - \alpha_{b0}^{(0)}}{\epsilon_+} - \frac{2i\hbar}{\mathcal{P}\epsilon_+} [\gamma_{ab} - i(\omega_0 - \omega - kv)] \beta_{-1}^{(1)*} \quad (42)$$

B. Second-Order Solution: Quadratic Response to Weak Field

The solution to second order in ϵ_- is obtained by solving Eq. (26) with $p=2$. As we are interested only in the coefficients $\beta_0^{(2)}$ and $\alpha_{a0}^{(2)} - \alpha_{b0}^{(2)}$, we have to solve these equations only for $n=0$. One then gets the following system:

$$\gamma_a \alpha_{a0}^{(2)} + i \frac{\mathcal{P}\epsilon_+}{2\hbar} (\beta_0^{(2)} - \beta_0^{(2)*}) = -i \frac{\mathcal{P}}{2\hbar} (\beta_{-1}^{(1)} - \beta_{-1}^{(1)*}), \quad (43a)$$

$$\gamma_b \alpha_{b0}^{(2)} - i \frac{\mathcal{P}\epsilon_+}{2\hbar} (\beta_0^{(2)} - \beta_0^{(2)*}) = i \frac{\mathcal{P}}{2\hbar} (\beta_{-1}^{(1)} - \beta_{-1}^{(1)*}), \quad (43b)$$

$$[\gamma_{ab} + i(\omega_0 - \omega + kv)] \beta_0^{(2)} + i \frac{\mathcal{P}\epsilon_+}{2\hbar} (\alpha_{a0}^{(2)} - \alpha_{b0}^{(2)}) = -i \frac{\mathcal{P}}{2\hbar} (\alpha_{a1}^{(1)} - \alpha_{b1}^{(1)}) \quad (43c)$$

The right-hand sides of these equations contain the first-order coefficients $\beta_{-1}^{(1)}$ and $\alpha_{a1}^{(1)} - \alpha_{b1}^{(1)}$ given by

Eqs. (39) and (42). The solution of the system (43) as a function of these quantities is straightforward. In particular the coefficients $\beta_0^{(2)}$ and $\alpha_{a0}^{(2)} - \alpha_{b0}^{(2)}$ are linked by the following relation, obtained by subtracting Eqs. (43a) and 43b):

$$\alpha_{a0}^{(2)} - \alpha_{b0}^{(2)} = -i \frac{\mathcal{P}\epsilon_+}{\hbar\gamma} (\beta_0^{(2)} - \beta_0^{(2)*}) - i \frac{\mathcal{P}}{\hbar\gamma} (\beta_{-1}^{(1)} - \beta_{-1}^{(1)*}). \quad (44)$$

We are now in possession of all the equations needed to calculate the physical quantities of interest $G_{-}^{(1)}(v, \omega, I)$, $G_{+}^{(2)}(v, \omega, I)$, and $N^2(v, \omega, I)$ given by Eqs. (31), (33), and (37). We are thus able to proceed to the study of these quantities which will provide a complete description of the main features of saturated-absorption phenomena.

V. POWER ABSORBED ON PROBE FIELD AS FUNCTION OF ATOMIC VELOCITY

In a saturated-absorption experiment, one is essentially concerned with the total power absorbed from the weak-return wave by the atomic medium. This power is obtained by integrating the function $G_{-}(v, \omega, I)$ over the velocity distribution according to Eq. (34). In order to get a deep insight into the physical phenomena involved in saturated absorption we will, before performing this integration, study first the function $G_{-}(v, \omega, I)$ itself which represents the rate of energy absorption by each ensemble of atoms with a given axial velocity.

$G_{-}(v, \omega, I)$ is, to lowest order in ϵ_- , given by the relation (31) with $\beta_{-1}^{(1)}$ determined by Eq. (39). If one replaces in this last equation $\alpha_{a0}^{(0)} - \alpha_{b0}^{(0)}$ by its expression (19b), one readily gets

$$G_{-}^{(1)}(v, \omega, I) = \left[-\frac{\omega \mathcal{P}^2 \epsilon_-^2}{2\hbar \gamma_{ab}} \right] [N_0] [W(v)] \left[1 - \frac{I^2 \gamma_{ab}^2}{\gamma_{ab}^2 + (\omega_0 - \omega + kv)^2 + I^2 \gamma_{ab}^2} \right] \left[\frac{\gamma_{ab}^2}{\gamma_{ab}^2 + (\omega_0 - \omega - kv)^2} \right] [1 - I^2 \text{Re } B(v, \omega, I)] \quad (45)$$

with $B(v, \omega, I)$ defined by relation (40). This expression is the product of six bracketed quantities, the physical meaning of which is quite clear. The first one recalls that the power absorbed from the probe field is merely proportional to the intensity ϵ_-^2 and the frequency ω of this field, as also to the square of the atomic dipole moment and to the relaxation time $1/\gamma_{ab}$ of this dipole. The second factor represents the population difference obtained at equilibrium when there is no light irradiation. It is a negative quantity if there is no population inversion in the medium, as is always the case in a saturated-absorption experiment. The third factor simply expresses that the rate of energy absorption by atoms with a given axial velocity v is proportional to the number of atoms corresponding to this ve-

locity in the Maxwellian distribution. The fourth factor expresses that the population distribution described by the two preceding terms is reduced by the saturation of the medium under the action of the pump field. As already noticed above, this factor describes the hole burnt in the Maxwellian distribution at $kv = \omega - \omega_0$ by the saturating field. The fifth factor is a Lorentzian term resonant when the condition $kv = \omega_0 - \omega$ is fulfilled. This relation corresponds to the matching between the atomic eigenfrequency ω_0 and the Doppler-shifted frequency of the probe field propagating in the reverse direction, $\omega_- = \omega + kv$. In other terms, the fifth factor in Eq. (45) merely expresses the resonant condition for the absorption of the probe field by atoms with axial velocity v .

The product of the five quantities described above, which we call $G_{r-}^{(1)}(v, \omega, I)$, corresponds exactly to the result given for the absorption of energy by the rate-equations (or "hole-burning") model; in this model indeed, the power absorbed from the probe field is merely proportional to the population difference in the presence of the strong saturating field [product of second to fourth factor in Eq. (45)] and to the Lorentzian absorption function centered at the Doppler-shifted atomic frequency [fifth factor in Eq. (45)]. It is thus the sixth term of Eq. (45), namely $1 - I^2 \text{Re}B(v, \omega, I)$, which takes into account all the phase relationships between atomic dipoles that are disregarded in the simple rate-equation formalism and which hence contains all the difference between the hole-burning model and ours. In order to emphasize this point, we will write Eq. (45) in the more compact form

$$G_{r-}^{(1)}(v, \omega, I) = G_{r-}^{(1)}(v, \omega, I) [1 - I^2 \text{Re}B(v, \omega, I)], \quad (46)$$

and before studying the variations of $G_{r-}^{(1)}(v, \omega, I)$ we will recall briefly the shape of the absorption curves versus velocity given by the rate-equations model.

A. Results Derived from Hole-Burning Model

Figure 2 shows the function $G_{r-}^{(1)}(v, \omega, I)/W(v)$ for different values of the frequency detuning $\omega_0 - \omega$. This function has been plotted for a value $I^2 = 30$ of the saturation parameter. The curves have been normalized by setting equal to unity the positive product of the two first factors in Eq. (45) (let us recall that N_0 is negative), so that they represent essentially the product of the Lorentz-shaped functions centered at $kv = \pm(\omega_0 - \omega)$ in the fourth and fifth brackets of this equation. In order to put into evidence the effect of saturation by the pump field, we have also plotted in dotted lines, for each value of the detuning, the corresponding absorption curve in the case of no pump field present ($I = 0$), that is the simple Lorentzian function

$$\gamma_{ab}^2 [\gamma_{ab}^2 + (\omega_0 - \omega - kv)^2]^{-1}.$$

When the detuning $\omega_0 - \omega$ is important [Fig. 2(a)], the absorption exhibits a strong resonance around $kv = \omega_0 - \omega$. The resonance is then practically not affected by saturation because the pump field ϵ_+ interacts essentially with atoms of opposite velocity $kv = -(\omega_0 - \omega)$ and does not appreciably perturb the atoms coupled with the probe field [resonances $kv = \omega_0 - \omega$ and $kv = -(\omega_0 - \omega)$ are well resolved as long as the detuning $\omega_0 - \omega$ is much larger than the width $\gamma_{ab} I$ of the pump-field saturated resonance]. When $\omega_0 - \omega$ decreases and becomes of the order of or smaller than $\gamma_{ab} I$ [Figs. 2(b) and 2(c)] the resonance, always centered around $kv = \omega_0 - \omega$, gets smaller. This decrease comes from the fact that

the hole burnt by the pump field begins to overlap the Lorentzian absorption curve of the probe field. This effect becomes the most important when $\omega_0 - \omega = 0$ [Fig. 2(d)]. The resonance observed on the absorption of the weak field is now centered at $kv = 0$; it is then considerably attenuated by the saturation of the same class of atoms under the action of the pump field. We will now study how these simple and well-known results are modified when one describes correctly the coupling between the atomic medium and the electromagnetic fields.

B. Absorption of Probe Field in Nonresonant Case ($\omega_0 - \omega \neq 0$): Appearance of New Raman and Rayleigh Processes

We have plotted on Fig. 3 the exact function $G_{r-}^{(1)}(v, \omega, I)/W(v)$ given by Eq. (45) and normalized as before. The curves have been plotted in the particular case¹⁸ $\gamma_a = \gamma_b = \gamma_{ab} = \gamma$ and for the same saturation parameter $I^2 = 30$ and detuning values $\omega_0 - \omega$ as was done in Fig. 2 for the "hole-burning" model. For important detuning [$\omega_0 - \omega \gg \gamma_{ab} I$,

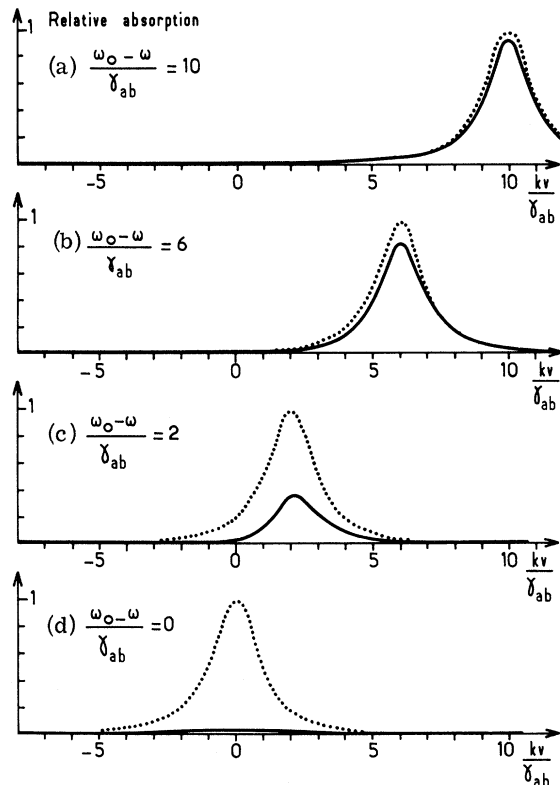


FIG. 2. Probe absorption vs velocity obtained from rate equations. Each solid curve represents the function $G_{r-}^{(1)}(v, \omega, I)/W(v)$ for a saturation parameter $I^2 = 30$ and for a given value of the detuning $(\omega_0 - \omega)/\gamma_{ab}$. The dotted curves, drawn for comparison, indicated for the same values of the detuning the unsaturated absorption of the probe ($I = 0$). The curves have been normalized by setting equal to unity the maximum value of this unsaturated absorption.

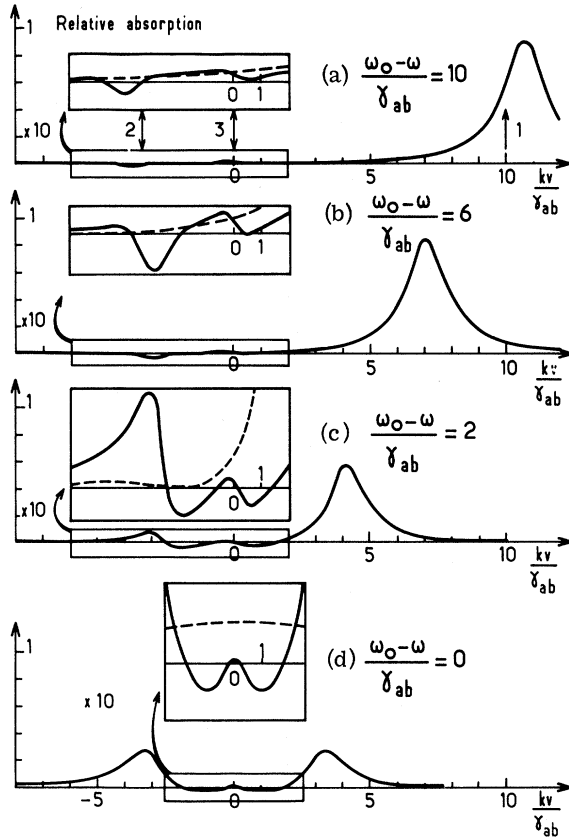


FIG. 3. Probe absorption vs velocity obtained from our complete model. The solid curves represent the function $G^{(1)}(\nu, \omega, I)/W(\nu)$; they are drawn (in the case $\gamma_a = \gamma_b = \gamma_{ab} = \gamma$) for the same saturation parameter and detuning values as in Fig. 2 for the rate-equations model and normalized in the same way. (a) Three resonant features near $kv = \omega_0 - \omega$, $kv = -\frac{1}{3}(\omega_0 - \omega)$, and $kv = 0$ are indicated by arrows 1, 2, and 3. (b) and (c) show how these features merge into each other to produce at resonance [Fig. 3(d)] a split line shape with two symmetric amplifying zones for slowly moving atoms. In order to make clearly apparent the new features of the curves, the parts of interest have been magnified by a factor of 10 in an insert above each curve. The dashed-line curve in each insert gives, for comparison, the corresponding probe absorption in the rate-equations model.

Fig. 3(a)] we notice that the absorption of the probe field exhibits again a strong resonance about the value $kv = \omega_0 - \omega$ indicated by arrow 1 on Fig. 3(a). This resonance is slightly shifted from the position given by the hole-burning theory [compare with the corresponding resonance on Fig. 2(a)]. This shift can be understood as a light shift⁶ induced on the corresponding atoms by the strong nonresonant pump field. As a new result, one can also observe other resonant features in the curve corresponding to atoms whose velocity lies near $kv = -\frac{1}{3}(\omega_0 - \omega)$ or $kv = 0$. These resonances come from the energy denominators $\gamma_{ab} - i(\omega_0 - \omega + 3kv)$ and $\gamma_a - 2ikv$,

$\gamma_b - 2ikv$ which appear in the expressions (40) and (41) of $B(\nu, \omega, I)$ and $f(\nu)$. Whereas the large resonance centered at $kv = \omega_0 - \omega$ corresponds essentially to the simple absorption of the probe photon by atoms of matched velocity, the new resonant features observed on this curve can easily be understood as essentially nonlinear Raman and Rayleigh processes involving both pumps and probe photons.

(a) The atoms may be excited from level b to a by absorption of two photons of the pump field followed by the stimulated reemission of one photon of the probe field [see Fig. 4(a) which symbolizes this process]. The following frequency-matching relationship in the atom rest frame must then be fulfilled:

$$2(\omega - kv) - (\omega + kv) = \omega_0. \quad (47)$$

This "Raman-type" condition precisely reduces to $kv = -\frac{1}{3}(\omega_0 - \omega)$. The corresponding resonance observed on Fig. 3(a) (arrow 2) appears as a decrease in the absorption, the function $G^{(1)}(\nu, \omega, I)$ changing its sign and taking negative values: As the process described above is related to a stimulated emission of light in the probe field, one understands that negative absorption, that is in fact amplification, may occur for the corresponding class of atoms.

(b) On the other hand, an atom may, without changing its energy level, absorb one photon in one of the fields and reemit another photon in the second field [the corresponding processes are symbolized on Fig. 4(b)]. The following frequency-matching relationship must then be fulfilled in the atom rest frame:

$$\omega - kv = \omega + kv. \quad (48)$$

This Rayleigh-type condition reduces to $kv = 0$, and

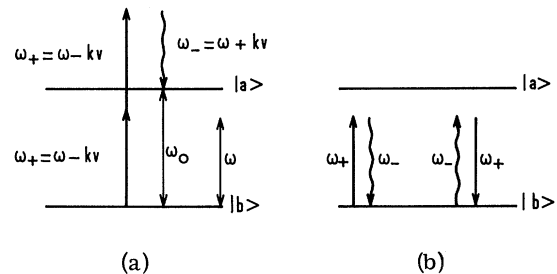


FIG. 4. Diagrams symbolizing the nonlinear processes involved in saturated absorption far off resonance [$(\omega_0 - \omega)/\gamma_{ab} \gg 1$]. (a) Representation of the Raman transition corresponding to the absorption of two pump photons at frequency $\omega_+ = \omega - kv$ and the reemission of one probe photon at frequency $\omega_- = \omega + kv$. (b) Representation of the "Rayleigh process" in which one photon of the probe is emitted (or absorbed) while one pump photon is absorbed (or emitted). Pump and probe photons are, respectively, symbolized by straight and wavy lines.

we thus understand the advent of the new resonant feature indicated by arrow 3 on Fig. 3(a). One must notice that the probe-field photon may in this process be either absorbed or emitted (while the pump field photon is emitted or absorbed). The calculation shows that the former process dominates for kv slightly negative whereas the reverse is true if kv is slightly positive. As a consequence, the resonant feature observed near $kv = 0$ exhibits a dispersionlike shape. We must also remark that even for a strong saturating field ($I^2 = 30$), the nonlinear effects quoted above¹⁹ are very small compared to the large resonant "one-photon" effect observed near $kv = \omega_0 - \omega$, (in order to make these effects clearly observable, we have magnified in Fig. 3 by a factor of 10 the regions of interest in the absorption curve) so that there is after all, in the nonresonant case $|\omega_0 - \omega| > \gamma_{ab} I$, only small quantitative discrepancies between curves of Figs. 2(a) and 3(a). However, if the frequency mismatch $\omega_0 - \omega$ is decreased, the different resonances described above will begin to overlap each other as is shown in Figs. 3(b) and 3(c). Then the Raman and Rayleigh processes will interfere with the one-photon process, and it will become impossible to separate any more all these processes from each other. The exact computation of formula (45) shows that the probe-field absorption curve then evolves into a structure drastically different from the one predicted by the hole-burning model.

C. Absorption of the Probe Field in the Resonant Case ($\omega_0 = \omega$)

Figure 3(d) shows the absorption curve versus velocity when frequency ω is tuned on the atomic resonance line ($\omega_0 = \omega$). Instead of observing one simple strongly saturated-absorption resonance curve centered at $kv = 0$, as predicted by the hole-burning model [see Fig. 2(d)], the absorption line shape develops into a split resonant feature symmetric around $kv = 0$. For atoms whose Doppler

shift kv lies within a few natural widths around zero, one furthermore observes a reversal of the sign of the absorption, corresponding to a stimulated emission on the probe field [see insert in Fig. 3(d)]. This amplification phenomenon is quite unexpected since it occurs in a two-level atomic system not subjected to population inversion. It is an effect essentially due to the pump-field saturation of the medium which appears, in the limit $\omega_0 = \omega$, as a "memory" of the Raman and Rayleigh stimulated emission processes described above in the nonresonant case. One can in particular see on Figs. 3(b) and 3(c) how the absorption curve evolves continuously from a situation where the two resonant features marked by arrows 2 and 3 are well resolved to a single structure where these resonances merge into each other to produce two amplification regions symmetric around $kv = 0$. These two regions are separated from each other by a small "absorption bump" corresponding to the axially motionless atoms for which the amplification effect never occurs.

We have plotted on Fig. 5 the same absorption versus velocity curves at resonance, but for various values of the saturation parameter I^2 . One can see from direct inspection of these curves, that the splitting of the two absorption peaks increases with saturation power and is roughly proportional to the pump-field amplitude I . On the other hand, the amplification phenomenon just described above occurs only for sufficiently large pump-field intensities ($I^2 > 3$). Let us also notice that the amplitude of this emission feature, which is always rather small compared to the absorption peaks, goes through a maximum as the saturation parameter increases and finally tends to zero when I^2 becomes very large.

All these new effects, which result from exact computation of formula (45) may, at least qualitatively, be understood if one makes reference to some

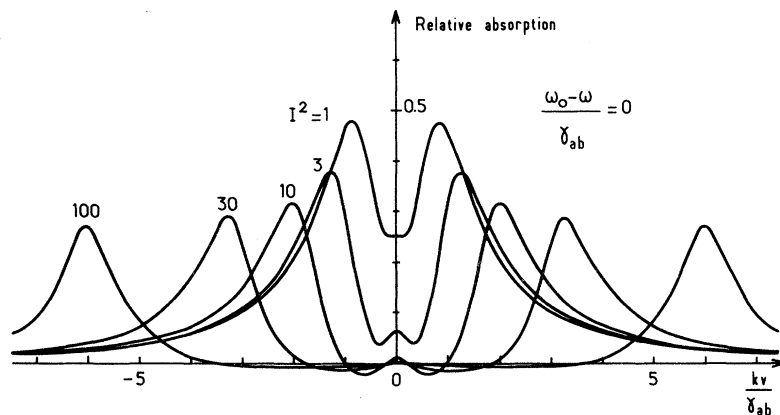


FIG. 5. Relative probe absorption vs velocity at resonance [$(\omega_0 - \omega / \gamma_{ab} = 0)$]. Each curve is drawn for a given value of the saturation parameter I^2 . The splitting of the resonances is seen to be proportional to I . The negative part of the curves correspond to the amplification effect described in the text. This phenomenon occurs only for strong-enough saturation ($I^2 > 3$). Its amplitude goes through a maximum when I is increased and tends to zero when saturation becomes very large. The area of the negative part of the curve is shown to decrease as $1/I$ when I tends to infinity. The curves are drawn in the case $\gamma_a = \gamma_b = \gamma_{ab} = \gamma$.

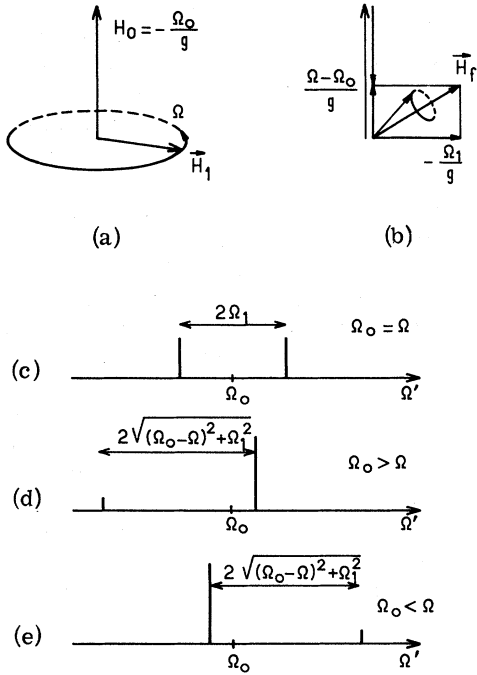


FIG. 6. "Dynamic Stark splitting" explained in a two-level system which is described as a spin $\frac{1}{2}$. (a) Static field H_0 and pump field H_1 seen in the laboratory frame. (b) Same fields in the rotating frame. The magnetic field H_f is now time independent and the spins precess around it, at frequency $[(\Omega_0 - \Omega)^2 + \Omega_1^2]^{1/2}$. (c), (d), and (e) Spectrum of probe resonances at frequencies $\Omega' = \Omega \pm [(\Omega_0 - \Omega)^2 + \Omega_1^2]^{1/2}$ for different values of pump detuning.

well-known effects in radiofrequency spectroscopy experiments.

D. Connection with rf Spectroscopy

It is well known in rf spectroscopy that the irradiation of an atomic system with a saturating pump field quasiresonant for a given transition drastically changes the absorption spectrum of a weak probe field tuned to a line sharing at least one common level with the pump-field transition. The absorption line of the probe field is then generally split into two lines whose frequency separation depends upon the pump-field amplitude and frequency. This effect, known as dynamic Stark splitting in microwave spectroscopy,⁷ is also observable and easily understood in the case of magnetic resonance on a two-level system.²⁰ Such a system can always be described as a spin one-half immersed in a static magnetic field \vec{H}_0 and irradiated by two rotating magnetic fields $\vec{H}_1(t)$ (pump field) and $\vec{h}_1(t)$ (probe field). The relative disposition of the static and pump fields is shown on Fig. 6(a). The pump \vec{H}_1 (frequency Ω) is rotating in a plane perpendicular to \vec{H}_0 . We will call $\Omega_0 = -gH_0$ the Larmor frequency of the spins with a gyromagnetic ratio g . In order

to study the position of the probe-field absorption lines, we will first analyze the motion of the spins driven by the pump field by making use of the rotating frame associated with \vec{H}_1 [Fig. 6(b)]. In this frame, the pump field becomes time independent and the atoms experience a static effective field

$$H_f = -g^{-1}[(\Omega_0 - \Omega)^2 + \Omega_1^2]^{1/2},$$

where Ω_1 is the amplitude of the pump field in frequency units. Therefore, the spins will in such a frame precess around H_f at the Rabi nutation frequency gH_f [see Fig. 6(b)]. As a result, the global evolution of the spins driven by the pump field may be analyzed in the laboratory frame as a superposition of the precession of the rotating frame at frequency Ω and of the Rabi flipping nutation. One thus finds in the precession of the spins two Fourier components at frequencies $\Omega \pm [(\Omega_0 - \Omega)^2 + \Omega_1^2]^{1/2}$. The probe $h_1(t)$ will consequently be absorbed when its frequency Ω' will coincide with one of these two eigenfrequencies, that is when the resonant condition

$$\Omega' = \Omega \pm [(\Omega_0 - \Omega)^2 + \Omega_1^2]^{1/2} \quad (49)$$

will be fulfilled. When the pump field is resonant ($\Omega_0 = \Omega$), the two lines thus obtained are symmetric about the frequency $\Omega_0 = \Omega$, their splitting being equal to $2\Omega_1$ [see Fig. 6(c)]. When the pump field is no longer resonant ($\Omega_0 \neq \Omega$), the intensities of the two lines become unequal. It is easy to understand that the larger one is always the closer to Ω_0 , as it must of course continuously evolve into the resonance line of the unperturbed spin system when the detuning of the pump field $\Omega_0 - \Omega$ becomes very large. It is thus clear that the larger resonance of the doublet is associated with the plus sign in Eq. (49) if $\Omega_0 > \Omega$ [the shift of this resonance is then positive, see Fig. 6(d)] whereas it is associated with the minus sign in Eq. (49) if $\Omega_0 < \Omega$ [the shift of this larger resonance is then negative, see Fig. 6(e)].

Let us now return to our saturated-absorption problem. In the rest frame of atoms with axial velocity v , we are exactly in the situation described above. The atomic system experiences a very strong pump field at a Doppler-shifted frequency $\omega_+ = \omega_0 - kv$ (we suppose again here that $\omega = \omega_0$). This strong pump field splits the atomic resonance absorption line, so that the probe field running in the opposite direction becomes now resonant if its frequency ω_- is given in the atom rest frame by the right-hand side of Eq. (49) in which one has to replace Ω by $\omega_+ = \omega_0 - kv$, $\Omega_0 - \Omega$ by $\omega_0 - \omega_+ = kv$, and Ω_1 by $\varphi \epsilon_+ / \hbar = I(\gamma\gamma_{ab})^{1/2}$. The resonance condition is then in the atom rest frame:

$$\omega_- = \omega_0 - kv \pm (k^2 v^2 + I^2 \gamma\gamma_{ab})^{1/2}. \quad (50)$$

If one remembers that ω_- is the Doppler-shifted

frequency $\omega_0 + kv$ of the weak return wave, one finally gets

$$2kv = \pm (k^2 v^2 + I^2 \gamma \gamma_{ab})^{1/2}; \quad (51)$$

Eq. (51), with a plus sign in it, yields the positive kv solution

$$kv = I \left(\frac{1}{3} \gamma \gamma_{ab}\right)^{1/2}, \quad (52a)$$

which corresponds to the matching of the positive probe-field Doppler shift ($kv > 0$) with the positive shift associated to the larger resonance of the Stark doublet [see Fig. 6(d) corresponding to a positive $\Omega_0 - \Omega = kv$ value]. On the other hand, Eq. (51) with a minus sign before the radical leads to the negative solution

$$kv = -I \left(\frac{1}{3} \gamma \gamma_{ab}\right)^{1/2}, \quad (52b)$$

which corresponds to the matching of the negative probe-field Doppler shift ($kv < 0$) with the negative shift associated again to the larger resonance of the doublet [see Fig. 6(e) corresponding to a negative $\Omega_0 - \Omega = kv$ value].

We thus understand the existence in the absorption curve of two symmetric absorption peaks separated by a splitting proportional to I . In short, the dynamic Stark splitting induced by the pump field in the atomic rest frame reveals itself by a splitting of the absorption curve versus velocity for the weak probe field; the atoms which most strongly absorb this probe field are those for which the shift due to the Stark splitting is compensated by the Doppler shift of the return wave.²¹ The above description of the phenomenon, although it explains well the gross features of the curves in Fig. 5, is however not precise enough to account for the fine structure exhibited by the curves for slowly moving atoms. One nevertheless understands clearly that a deep decrease of the absorp-

tion must occur between the two peaks, which follows from the fact that the pump field not only saturates the population difference for these atoms but also "pushes" up and down the atomic eigenfrequencies. This explains why the weak return field is less absorbed by these classes of atoms as would be the case if the atomic frequencies were not modified by the Stark splitting [compare for example the curves in solid and dashed lines in the insert of Fig. 3(d), which give the absorption for slowly moving atoms in our calculation as compared to the hole-burning model].

So far, we do not yet understand how it happens that the absorption is so strongly saturated for these slow atoms that they even amplify the probe field. Another classical effect in rf spectroscopy, the amplification by saturated absorption^{22,23} may however be invoked in order to clarify this new interesting phenomenon. This effect is related to the absorption of an amplitude-modulated rf field by an atomic two-level system. Let us consider such an atomic medium attacked by an rf field inducing transitions between the levels. We have plotted on Fig. 7(a) the characteristic curve which represents the output intensity versus the input rf intensity I^2 sent on the medium.²³ This curve starts for weak rf power with a slope smaller than unity, which merely expresses the fact that a fraction of the incident power is absorbed in the medium; for strong rf fields, on the other hand, the characteristic slope becomes equal to unity, which corresponds to the fact that any incremental power sent on the medium is entirely transmitted when saturation is reached. Suppose now that the input field is amplitude modulated at a frequency δ . This modulation entails the appearance of two symmetric sidebands at frequencies $\omega + \delta$ and $\omega - \delta$ in the spectrum of the rf field. If δ is a

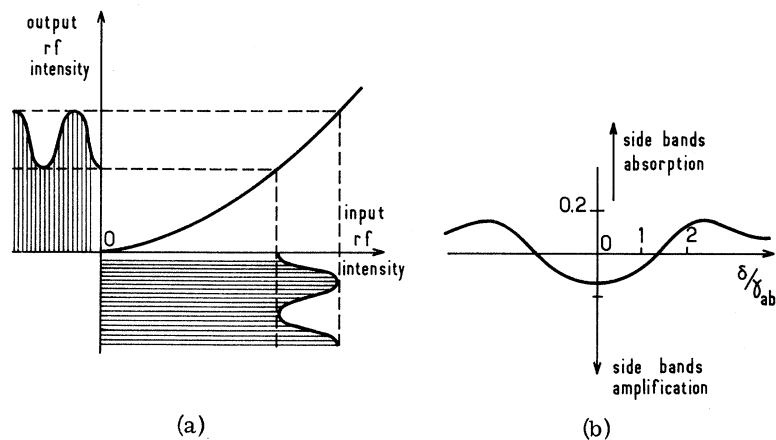


FIG. 7. Amplification by resonance saturation. (a) Transmission characteristic showing output vs input rf intensity for a two-level resonant atomic system. The characteristic slope, smaller than one for weak input power, tends to unity when the medium is saturated. If the signal is modulated at not too large a frequency δ , the atoms can "follow," and the modulation depth in the linear asymptotic part of the characteristic is shown to be fully restituted at the output, whereas the carrier signal undergoes some attenuation. This corresponds to amplification of the sidebands (from Ref. 23). (b) Curve showing the relative sidebands amplification or absorption as a function of δ for a value $I^2 = 3$ of the saturation parameter. The unsaturated absorption of the system at resonance is taken as unity (from Ref. 22).

small-enough modulation frequency, the output power can follow almost adiabatically the variations of the input field. It appears immediately, in the saturation region of the characteristic, that the output-modulation depth is about the same as the input one, while the "carrier" amplitude is somewhat reduced [see Fig. 7(a)]. In terms of Fourier analysis, the relative enhancement of the modulation depth results in an amplification of both sidebands at frequencies $\omega + \delta$ and $\omega - \delta$. We must notice that this effect which has been experimentally observed,²² occurs only in the case of strong-enough saturation by the carrier field so that the modulation takes place in the linear asymptotic part of the characteristic. On the other hand, the frequency δ has to be sufficiently small for the atoms to be able to follow the modulation of the field. When δ becomes of the order of the power-broadened linewidth $\gamma_{ab}I$, the effect reverses its sign and absorption actually occurs on the sidebands. The sidebands amplification versus modulation frequency δ as it results from the calculation of Ref. 22 has been plotted on Fig. 7(b) for a value $I^2 = 3$ of the saturation parameter. We notice that the absorption in the wings presents two resonant peaks for two symmetric values of δ , which are nothing but the dynamic Stark doublet already described above.

Let us now come back to our optical problem. The atoms with axial velocity v experience in their rest frame the pump field at frequency $\omega_+ = \omega_0 - kv$. The weak-return field at frequency $\omega_- = \omega_0 + kv$ may be considered as a sideband separated from the carrier by the frequency $2kv$. If this frequency is small enough compared to the power-broadened linewidth $\gamma_{ab}I$, we understand that an amplification process similar to the one described above can take place. This phenomenon corresponds to the negative part of the curves of Fig. 5. It is clear that this effect can occur only for strong-enough saturation by the pump field and for sufficiently small axial velocities. We must however notice that the analogy mentioned here between the rf amplification effect and the optical one is only qualitative.²⁴ In particular, the weak probe field in the saturated-absorption experiment corresponds to a unique sideband instead of two in the rf experiment. Thus, the em field "seen" by each atom of given velocity is not really an amplitude-modulated one. This explains some discrepancies between the features of the curves in Figs. 5 and 7(b). In particular, it may be shown from the equations given in Ref. 22 that a unique sideband is always attenuated if the mismatch frequency δ with the pump carrier field is small compared to γ_{ab} (slow modulation limit). This explains the small bump in curves of Fig. 5 for $kv = 0$ and the fact that the motionless atoms always absorb the

probe field.²⁵

VI. TOTAL POWER ABSORBED FROM PROBE FIELD AND SATURATED-ABSORPTION LINE SHAPE

We are now in a position to calculate the global power $G_-^{(1)}(\omega, I)$ absorbed from the probe field by the atomic medium. The total absorption is obtained [Eq. (34)] by integration over axial velocity of the functions $G_-^{(1)}(v, \omega, I)/W(v)$ plotted in Figs. 3 and 5 multiplied by the Maxwellian distribution $W(v)$. This integration may be performed with the use of the theorem of residues to yield explicit formulas for the line shape. As expressions obtained are very cumbersome, we will not give them here and rather discuss the equivalent results obtained by numerical integration on a computer. We will first study the case of an infinite Doppler width, which is the most relevant one for saturated-absorption experiments. We will then consider the case of finite Doppler width, for which an interesting phenomenon of global amplification on the return wave may occur.

A. Absorption in Infinite Doppler-Width Limit

In the limit of an infinitely broad Doppler distribution ($kv_m \gg \gamma_{ab}I, \gamma_{ab}$), $W(v)$ may be considered as a constant and the power $G_-^{(1)}(\omega, I)$ is merely proportional to the areas under the curves of Figs. 3 and 5. We have plotted on Fig. 8 the function $G_-^{(1)}(\omega, I)$ versus the detuning $\omega - \omega_0$ for the value $I^2 = 10$ of the saturation parameter. This function is normalized by setting equal to unity the unsaturated absorption of the probe ($I^2 = 0$). In dashed lines is also represented the quantity $G_{r_-}^{(1)}(\omega, I)$, obtained in the same way from the rate-equations theory [$G_{r_-}^{(1)}(\omega, I)$ may be shown to be a Lorentzian function, contrary to $G_-^{(1)}(\omega, I)$]. We can clearly see that the absorption of the probe field exhibits on both curves a strong decrease when the em field is tuned to the atomic frequency ω_0 : This is the well-known absorption-saturation phenomenon. However, we observe also on the figure that the saturation of the real absorption is less pronounced than predicted by the simple hole-burning model. This may be readily understood by comparison between the areas under the curves of Figs. 3 and 2. The probe absorption, with no pump field present, is merely proportional to the area under the dotted curves of Fig. 2; it is independent from the detuning $\omega - \omega_0$ since we consider for the present an infinitely broad Doppler distribution. This area gives also the asymptotic value of the probe absorption in the presence of the pump, for large values of the detuning. For $\omega = \omega_0$, the absorption is given by the area under the solid line curve of Fig. 2(d) in the hole-burning model and by the area under the curve of Fig. 3(d) in our theory. These areas are both smaller

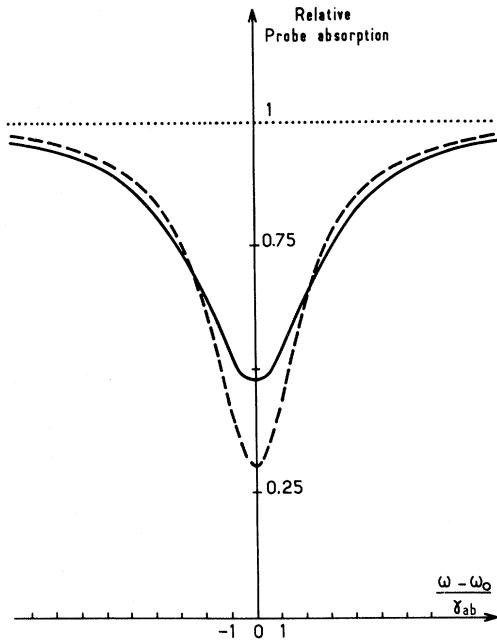


FIG. 8. Probe absorption line shape for infinite Doppler width. The solid curve gives the function $G_+^{(1)}(\omega, I)$ for a value $I^2=10$ of the saturation parameter. The dashed curve represents the corresponding line-shape function $G_{r-}^{(1)}(\omega, I)$ obtained in the hole-burning model. The dotted line indicates the unsaturated absorption $G_+^{(1)}(\omega, 0)$, which is constant in the infinite Doppler-width limit and whose value is taken as unity. The curves are drawn in the case $\gamma_a=\gamma_b=\gamma_{ab}=\gamma$.

than the one under the dotted curve of Fig. 2, but it appears immediately that the presence of the two side peaks on the curve of Fig. 3(d) makes the actual absorption larger than the one predicted from the hole-burning theory; in other terms, at resonance ($\omega = \omega_0$), the saturated medium absorbs more than predicted by rate equations. This is due to the fact that the saturating field which splits the atomic eigenfrequencies enhances the absorption of the probe field for classes of atoms corresponding to the wings of the velocity distribution, and this effect tends to oppose the classical effect of population saturation.

As a result, contrary to the predictions of rate equations, the saturation of the absorption can never be complete in the large-Doppler-width limit. This fact has already been pointed out in Ref. (8). On Fig. 9 we have plotted the relative decrease η of the absorption at the center of the resonance as a function of the saturation parameter. The solid-line curve, corresponding to the exact theory, tends asymptotically to a value of 62.5% for η , whereas the hole-burning model (dashed-line curve) predicts a 100% limit for the absorption saturation.⁵ Nevertheless, the two curves are close to each other for small values of I^2 , which

shows that rate equations are not too bad an approximation in this region.

B. Absorption for Finite Doppler Widths: Saturation of Doppler Width and Possibility of Global Amplification of Probe Field

In the case of finite—and rather small—Doppler widths, the saturation of the absorption may on the contrary be stronger than predicted by rate equations, and the medium may even exhibit global amplification on the return wave. Such a result is obtained when the saturation of the medium by the pump is so important that the side absorption peaks of Fig. 5 are rejected outside the width of the Maxwellian velocity distribution. In this case of “Doppler-width saturation” corresponding to the condition

$$I(\gamma\gamma_{ab})^{1/2} \gg kv_m, \quad (53)$$

most of the atoms within the Maxwellian velocity distribution indeed amplify the return wave. This effect is roughly proportional to the area of the negative part in the curves of Fig. 5, which may be shown to decrease as $1/I$ when I is very large. The global-amplification effect will thus be the most important in the pump-intensity range we will define as moderately strong ($I^2 \approx 10$ to 100). Condition (53) then shows that the Doppler width must not be larger than a few times the homogeneous width. As an example, Fig. 10 shows in solid line the absorption function $G_+^{(1)}(\omega, I)$ for $I^2=100$ and a most probable velocity v_m given by $kv_m/\gamma_{ab}=2.2$. The scale is given by the dotted-line curve on the

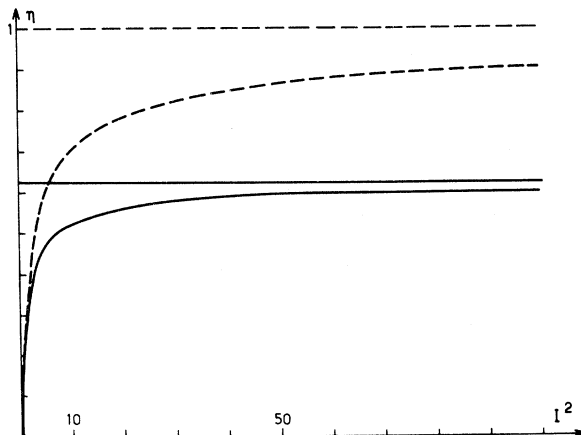


FIG. 9. Relative contrast of the saturated-absorption dip as a function of the saturation parameter, in the case of infinite Doppler width. The solid curve represents the function $\eta(I^2) = 1 - G_+^{(1)}(\omega_0, I)/G_+^{(1)}(\omega_0, 0)$ which tends asymptotically to $\eta(+\infty) = 0.625$. The dashed curve gives the corresponding contrast function in the hole-burning model, which tends to unity for strong saturation. The curves are plotted in the case $\gamma_a=\gamma_b=\gamma_{ab}=\gamma$.

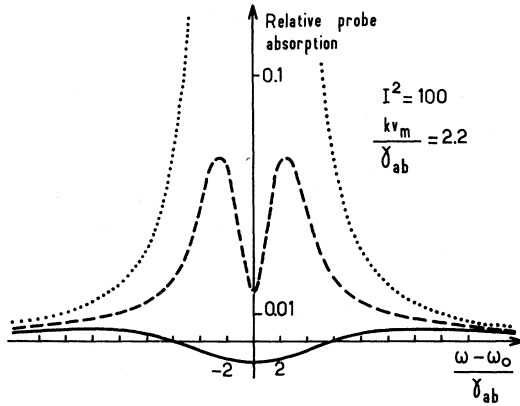


FIG. 10. Probe absorption line shape for finite Doppler width. The solid curve gives the function $G_-^{(1)}(\omega, I)$ for a value $I^2=100$ of the saturation parameter and for a Doppler width corresponding to $kv_m/\gamma_{ab}=2.2$. Note the negative absorption (amplification) for frequencies ω between $\omega_0 - 6\gamma_{ab}$ and $\omega_0 + 6\gamma_{ab}$. The dashed curve represents the corresponding line shape in the hole-burning model. No amplification is predicted by this model. The dotted curve corresponds to the unsaturated absorption ($I^2=0$) for the same Doppler width, normalized to unity at resonance. The curves are drawn in the case $\gamma_a = \gamma_b = \gamma_{ab} = \gamma$.

same figure which represents the unsaturated absorption of the probe ($I^2=0$) for the same Doppler width, normalized by setting equal to 1 the absorption at resonance ($\omega = \omega_0$). The amplification effect is observed within a range of frequencies around ω_0 with a relative amplitude of about 1%. We have also drawn for comparison in dashed line the curve which represents according to the hole-burning model the absorption of the probe for the same values of the parameters I^2 and kv_m . Of course, no amplification effect appears on this last curve.

Let us also notice that condition (53) implies that the radiative broadening of the resonance line by the pump field is larger than the Doppler width. It would however be false to conclude that the Doppler effect may be completely neglected in this case and that we are then in a situation equivalent to the one where the atoms are stationary ($kv=0$). In such a situation indeed, the absorption of the probe is merely equal to $G_-^{(1)}(0, \omega, I)$ which is always positive. Thus, the amplification effect described above essentially occurs for an intermediate range of Doppler widths.

This effect could be used in order to generate a unidirectional induced emission in a saturated-absorbing medium. Suppose for example that the pump field propagates along a given direction through a cell placed into a ring laser structure and containing an absorbing gas. If the pump-field intensity satisfies Eq. (53), the medium may

exhibit a net positive gain for an em field at frequency ω propagating in the direction opposite to the pump. Provided this gain overbalances the cavity losses, a return wave may be generated in the medium in this direction and eventually give rise to a stable laser oscillation. It is however obvious that the actual frequency of this oscillation will not necessarily be equal to the frequency ω of the pump. The exact study of such a laser emission thus implies the calculation of probe amplification at a frequency ω' slightly different from ω . This problem is outlined in the Appendix.

VII. SATURATION EFFECTS INDUCED BY PROBE FIELD

We have so far studied in detail the first-order response of the atomic system to the probe field, which is directly related to the absorption of this field by the medium. We will now briefly consider the second-order response of the system to this probe field which describes how the presence of the weak return wave reacts back on the saturating pump field and on the atomic population difference. This will allow us to clarify in particular a question unsolved by the first-order calculation about the origin of the energy absorbed or emitted on the probe field.

The physical second-order quantities of interest are $G_+^{(2)}(v, \omega, I)$ and $N^{(2)}(v, \omega, I)$ given by Eqs. (33) and (37), which represent, respectively, the modification of the energy absorbed on the pump field and the change in the population difference under the action of the probe field. Those quantities may be exactly computed from Eqs. (43) and (44), which give the coefficients $\alpha_{a0}^{(2)} - \alpha_{b0}^{(2)}$ and $\beta_0^{(2)}$. In particular, if one replaces in (44) these coefficients by their expressions as a function of $G_+^{(2)}(v, \omega, I)$ and $N^{(2)}(v, \omega, I)$ obtained from (33) and (37), one immediately gets the important relation

$$\frac{1}{2}\gamma\hbar\omega N^{(2)}(v, \omega, I) = G_-^{(1)}(v, \omega, I) + G_+^{(2)}(v, \omega, I), \quad (54)$$

which merely expresses the energy conservation in the whole system "atomic medium + pump and probe fields." It is indeed clear that the left-hand side of this equation represents the change, when the probe field is turned on, of the transition rate between atomic levels b and a times the energy $\hbar\omega$ of this transition. This term thus corresponds to the modification, due to the probe field, of the energy absorption rate by atoms with velocity v . It must hence be equal to the change in the global power delivered to these atoms by the probe and pump field, which is described by the right-hand side of Eq. (54).

In order to understand how the energy is actually exchanged between the three systems in interaction, we have computed the functions $G_+^{(2)}(v, \omega_0, I)/W(v)$ and $N^{(2)}(v, \omega_0, I)/W(v)$ in the resonant case ω_0

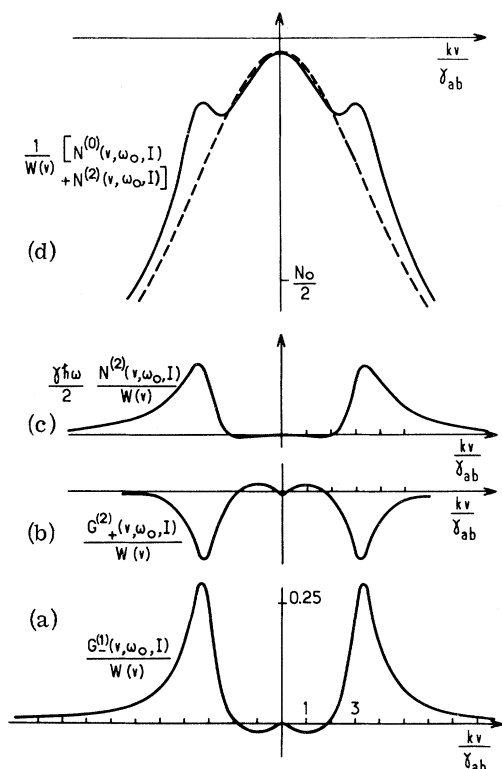


FIG. 11. Response of the system to second order in probe-field strength. (a) recalls for comparison the probe absorption vs velocity curve already represented in Fig. 3(d) for a value $I^2=30$ of the saturation. (b) gives in the same conditions the second-order correction $G_+^{(2)}(v, \omega_0, I)/W(v)$ to the pump-field absorption. Note that the amplification feature in the curve (a) corresponds to an increased absorption of the pump in the curve (b). (c) gives the second-order correction to the population difference which is proportional to the sum of the functions plotted on Figs. 11(a) and 11(b) [see Eq. (54)]. (d) gives the total population difference versus velocity under saturation by pump and probe fields for a value $I^2=30$ of the pump intensity and $\phi^2 \epsilon^2 / \hbar^2 \gamma \gamma_{ab} = 1$ of the probe strength. The effect of the probe saturation may be seen by comparison with the dashed curve which gives the population difference when only the pump is present. The different curves of the figure are drawn in the case $\gamma_a = \gamma_b = \gamma_{ab} = \gamma$.

$= \omega$. We have plotted on Fig. 11 the corresponding curves for a value $I^2=30$ of the saturation parameter (always in the case $\gamma_a = \gamma_b = \gamma_{ab} = \gamma$). On Fig. 11(a), we have plotted again the probe-field absorption curve $G_-^{(1)}(v, \omega_0, I)/W(v)$ for comparison purposes. Figure 11(b) represents, to the same scale, the change in the absorption rate of the pump field. For slowly moving atoms, we can see that the two curves $G_-^{(1)}(v, \omega_0, I)$ and $G_+^{(2)}(v, \omega_0, I)$ take practically opposite values: This means that the amplification of the probe field which takes place in this region is essentially obtained at the expense of the pump which experiences a further

attenuation when the probe field is turned on. For kv of the order of γI , on the other hand, we see that the absorption peaks of the probe field correspond to negative peaks in the $G_+^{(2)}$ curve. This means that the absorption of the pump field by the corresponding atoms is somewhat reduced when the probe is turned on. The energy delivered by the probe field does not yet flow integrally within the pump field, as we can notice that the amplitude of the peaks in Fig. 11(a) are approximately twice as large as those of Fig. 11(b). On Fig. 11(c) we have represented to the same scale the function

$$\frac{1}{2} \gamma \hbar \omega N^{(2)}(v, \omega_0, I) W(v)$$

which is, according to Eq. (54), merely the sum of the curves plotted in Fig. 11(a) and 11(b). We observe that the modification of the population difference is almost negligible for slowly moving atoms, whereas it becomes more important on the wings of the velocity distribution. As the atoms in this region absorb on the whole more energy when the probe field is turned on, we understand that a positive change of the population difference must then occur. We have finally plotted on Fig. 11(d) the curve

$$[N^{(0)}(v, \omega_0, I) + N^{(2)}(v, \omega_0, I)] / W(v)$$

which describes the total population difference under the saturation by both pump and probe fields. The curve is drawn for the same value $I^2=30$ as before and for a value $\phi \in \hbar \gamma \gamma_{ab} = 1$ of the probe-field amplitude. The dashed-line curve corresponds to the function

$$N^{(0)}(v, \omega_0, I) / W(v),$$

that is the Lorentzian hole-burnt by the pump field alone. When the probe is added, the shape of the hole (solid-line curve) is modified: Two symmetric peaks appear near its top, which are related to the global increase of em absorption by the corresponding atoms due to the presence of the probe. Let us emphasize that the shape thus obtained near the maximum of the $N(v)$ function is very similar to the structure predicted by high-intensity gas-laser theories¹¹⁻¹³ in the bottom of the population inversion curve versus velocity. The oscillations which develop in the bottom of this curve are related to population-ringing effects occurring for slowly moving atoms.¹³ The similar effect described in this paper for saturated absorption is linked, as we have shown above, to the dynamic Stark splitting produced by the pump field in the atom rest frame.

CONCLUSION

We have given in this paper a detailed description of the saturated-absorption phenomenon in the quasi-running-wave situation. We have put

into evidence some new effects which may become important for large values of the pump intensity and which are not accounted for by rate-equations theory. The most striking of these effects is the possibility of amplification of the weak-probe wave. These new phenomena essentially follow from the fact that the pump field not only saturates the populations but also coherently drives the atomic dipoles of the medium, which in particular entails the modification of the atomic eigenfrequencies. From this point of view, the present study appears as a special case of the general problem dealing with the interaction between a weak monochromatic wave and an atomic system whose eigenstates have been renormalized by the coupling with a strong em field. As was pointed out in various publications,²⁶ this problem might also be approached by considering that the weak field is absorbed by the whole system made of the atomic medium and the quantized pump field in interaction ("dressed-atom" formalism). Such a point of view would allow to interpret, in a more systematic way than was done in the present paper, all the predicted effects in terms of elementary processes involving real or virtual exchange of photons between the atoms and the em fields.

Let us finally summarize the conditions of validity of our theory. First, since we have described the em fields as plane waves, we have overlooked all transit time problems so that our study applies to situations in which the atomic mean free path is smaller than the transverse dimensions of the actual probe and pump light beams. Second, as we have given a classical description of the em fields as well as of the atomic motion, our model cannot deal with recoil effects which may affect the line shape.²⁷ Third, our description of relaxation does not take into account the velocity changing collisions which would couple together atomic ensembles of different v values. In order to overcome these limitations, it would be useful to quantize in the theory not only the em fields as was already suggested above, but also the external degrees of freedom of the atoms.²⁸

We must at last notice that we have here re-

stricted our attention to the absorption of the probe field by the atomic system. The same theory would of course allow the study of its dispersion properties by considering the real part of the atomic susceptibilities instead of their imaginary part.

ACKNOWLEDGMENTS

The authors are indebted to Professor C. Cohen-Tannoudji for helpful discussions. They are also happy to thank Dr. D. Spanjaard and Dr. L. Potier for their kind assistance with the computer work.

APPENDIX: EXTENSION OF THE THEORY TO FREE-FREQUENCY PROBE FIELD

As we were, in this paper, primarily interested in the description of saturated-absorption phenomena, we have limited our calculations to a probe field with the same frequency ω as the pump field. This limitation is however not a fundamental one, and it is easy to generalize the theory to the case of a probe field with a frequency ω' different from ω . Furthermore, the probe field may be allowed to propagate either in the same direction as the pump field²⁹ or in the opposite direction. We will in this Appendix give the outline of the theory applied to this general situation and obtain an explicit expression for the probe-field absorption.

The pump and probe fields are now defined by their frequency ω and ω' and their wave vectors $\vec{k} = (\omega/c)\vec{u}$ and $\vec{k}' = (\omega'/c)\vec{u}'$, where \vec{u} and \vec{u}' are unit vectors defining the sense of propagation along the z axis. Both frequencies ω and ω' are supposed to be quairesonant with the atomic frequency ω_0 .

The equations of motion for the density matrix are immediately deduced from Eqs. (17) by replacing, in the second bracketed expressions of the right-hand sides, the exponential factor $e^{i(\omega t + kz)}$ by $e^{i(\omega' t - k' z)}$. In this factor, k' is taken as positive if the probe field propagates in the same (positive) direction as the pump field, whereas k' is taken as negative if the probe field propagates in the reverse direction (as is the case in saturated-absorption experiments). One then has

$$\left(\frac{\partial}{\partial t} + v \frac{\partial}{\partial z}\right) \rho_{aa} = \lambda_a - \gamma_a \rho_{aa} - i \frac{\mathcal{P} \epsilon_+}{2\hbar} (\rho_{ab} e^{i(\omega t - kz)} - \rho_{ba} e^{-i(\omega t - kz)}) - i \frac{\mathcal{P} \epsilon_-}{2\hbar} (\rho_{ab} e^{i(\omega' t - k' z)} - \rho_{ba} e^{-i(\omega' t - k' z)}), \quad (55a)$$

$$\left(\frac{\partial}{\partial t} + v \frac{\partial}{\partial z}\right) \rho_{bb} = \lambda_b - \gamma_b \rho_{bb} + i \frac{\mathcal{P} \epsilon_+}{2\hbar} (\rho_{ab} e^{i(\omega t - kz)} - \rho_{ba} e^{-i(\omega t - kz)}) + i \frac{\mathcal{P} \epsilon_-}{2\hbar} (\rho_{ab} e^{i(\omega' t - k' z)} - \rho_{ba} e^{-i(\omega' t - k' z)}), \quad (55b)$$

$$\left(\frac{\partial}{\partial t} + v \frac{\partial}{\partial z}\right) \rho_{ab} = -(\gamma_{ab} + i\omega_0) \rho_{ab} - i \frac{\mathcal{P} \epsilon_+}{2\hbar} (\rho_{aa} - \rho_{bb}) e^{-i(\omega t - kz)} - i \frac{\mathcal{P} \epsilon_-}{2\hbar} (\rho_{aa} - \rho_{bb}) e^{-i(\omega' t - k' z)}. \quad (55c)$$

The solution of these equations to zero order in ϵ_- is obviously given by Eqs. (19a) and (19b), since it does not depend on the probe field. We can again look for a general solution taking the form of the power series in ϵ_- given by Eq. (23). The solution to order p may now be expanded in a form generalizing Eq. (24):

$$\rho_{jj}^{(p)}(z, t, v) = \sum_{nn'a} \alpha_{jnn'a}^{(p)} e^{i(nk-n'k')z} e^{iq(\omega-\omega')t} \quad (j=a, b), \quad (56a)$$

$$\rho_{ab}^{(p)}(z, t, v) = \sum_{nn'a} \beta_{nn'a}^{(p)} e^{i(nk-n'k')z} e^{iq(\omega-\omega')t} e^{-i(\omega t - kz)}. \quad (56b)$$

In the expression for the diagonal elements, we have taken into account the possibility of a slow modulation at frequency $\omega - \omega'$ and its harmonics. This modulation arises from the nonlinear coupling of the atomic medium to the two fields at frequencies ω and ω' . All modulations at frequencies $q\omega + q'\omega'$ with $q' \neq -q$, which also appear in the evolution of the diagonal matrix elements, may be neglected as the corresponding terms are divided by large energy denominators of the form $\gamma_j + i(q\omega + q'\omega')$ (secular approximation). The same kind of argument shows that the time dependence of the nondiagonal matrix element must be of the form $e^{iq(\omega-\omega')t - i\omega t}$ as indicated on Eq. (56b). On the other hand, the spatial dependence of the density matrix must now be expanded along the spatial Fourier components of both fields, which accounts for the term $e^{i(nk-n'k')z}$ in the above equations.

The coefficients $\beta_{nn'a}^{(p)}$ are related to the polarization of the medium by the following relation which generalizes Eq. (27):

$$P(z, t, v) = \mathcal{P} e^{-i(\omega t - kz)} (\beta_0^{(0)} + \sum_{pnn'a} \epsilon_-^p \beta_{nn'a}^{(p)} e^{i(nk-n'k')z} e^{iq(\omega-\omega')t}) + \text{c. c.} \quad (57)$$

The projection of the polarization onto the mode of the probe field is given by

$$P_-(z, t, v) = \mathcal{P} e^{-i(\omega' t - k' z)} \sum_p \epsilon_-^p \beta_{-1-1+1}^{(p)} + \text{c. c.} \quad (58)$$

so that the power absorbed on the probe field is given to lowest order by the following expression which generalizes Eq. (31):

$$G_-^{(1)}(v, \omega, \omega', I) = \omega' \mathcal{P} \epsilon_-^2 \text{Im}(\beta_{-1-1+1}^{(1)}). \quad (59)$$

The Fourier coefficients $\alpha_{nn'a}^{(p)}$ and $\beta_{nn'a}^{(p)}$ may be readily obtained if one replaces in Eq. (55) the density-matrix elements by their perturbation and Fourier expansion (23) and (56). One then gets a complete set of recurrent relations which allow the iterative calculation of these coefficients from the zero-order solution (19). The first-order susceptibility $\beta_{-1-1+1}^{(1)}$ can in particular be obtained from the equations

$$[\gamma_a + i(k - k')v - i(\omega - \omega')] \alpha_{a11-1}^{(1)} = -i \frac{\mathcal{P} \epsilon_+}{2\hbar} (\beta_{11-1}^{(1)} - \beta_{-1-11}^{(1)*}) - i \frac{\mathcal{P}}{2\hbar} \beta_0^{(0)}, \quad (60a)$$

$$[\gamma_b + i(k - k')v - i(\omega - \omega')] \alpha_{b11-1} = +i \frac{\mathcal{P} \epsilon_+}{2\hbar} (\beta_{11-1}^{(1)} - \beta_{-1-11}^{(1)*}) + i \frac{\mathcal{P}}{2\hbar} \beta_0^{(0)}, \quad (60b)$$

$$[\gamma_{ab} + i(\omega_0 - 2\omega + \omega') + i(2k - k')v] \beta_{11-1}^{(1)} = -i \frac{\mathcal{P} \epsilon_+}{2\hbar} (\alpha_{a11-1}^{(1)} - \alpha_{b11-1}^{(1)}), \quad (60c)$$

$$[\gamma_{ab} + i(\omega_0 - \omega') + ik'v] \beta_{-1-11}^{(1)} = -i \frac{\mathcal{P} \epsilon_+}{2\hbar} (\alpha_{a11-1}^{(1)*} - \alpha_{b11-1}^{(1)*}) - i \frac{\mathcal{P}}{2\hbar} (\alpha_a^{(0)} - \alpha_b^{(0)}). \quad (60d)$$

Taking the imaginary part of $\beta_{-1-1+1}^{(1)}$ obtained from these equations, one gets the expression of the power absorbed on the probe field in a form which generalizes Eq. (45):

$$G_-^{(1)}(v, \omega, \omega', I) = \left[-\frac{\omega' \mathcal{P}^2 \epsilon_-^2}{2\hbar \gamma_{ab}} \right] [N_0] [W(v)] \left[1 - \frac{I^2 \gamma_{ab}^2}{\gamma_{ab}^2 + (\omega_0 - \omega + kv)^2 + I^2 \gamma_{ab}^2} \right] \times \left[\frac{\gamma_{ab}^2}{\gamma_{ab}^2 + (\omega_0 - \omega' + k'v)^2} \right] [1 - I^2 \text{Re} B'(v, \omega, \omega', I)], \quad (61)$$

with

$$B'(v, \omega, \omega', I) = \frac{[\gamma_{ab} - i(\omega_0 - \omega' + k'v)] \{ [\gamma_{ab} - i(\omega_0 - \omega + kv)]^{-1} + [\gamma_{ab} + i(\omega_0 - \omega' + k'v)]^{-1} \}}{2f(v, \omega - \omega') + I^2 \gamma_{ab} \{ [\gamma_{ab} - i(\omega_0 - 2\omega + \omega' + 2kv - k'v)]^{-1} + [\gamma_{ab} + i(\omega_0 - \omega' + k'v)]^{-1} \}}, \quad (62)$$

$$f(v, \omega - \omega') = \frac{2}{\gamma} \frac{1}{[\gamma_a - i(k - k')v + i(\omega - \omega')]^{-1} + [\gamma_b - i(k - k')v + i(\omega - \omega')]^{-1}}. \quad (63)$$

The total power absorbed from the probe field is obtained as before by integrating over velocities

$$G_{-}^{(1)}(\omega, \omega', I) = \int_{-\infty}^{\infty} G_{-}^{(1)}(v, \omega, \omega', I) dv. \quad (64)$$

If one replaces in (61)–(63) ω' by ω and k' by $-k$ these equations reduce to (45), (40), and (41) which correspond to the saturated-absorption situation. We had seen in this case that at resonance ($\omega = \omega_0$) and for strong-enough saturation, an amplification of the probe return wave could take place. If we now keep ω at resonance but allow ω' to vary around ω_0 , we will find a range of frequencies ω' for which the probe field will be amplified. One can wonder if the amplification could be sufficient

so as to permit laser oscillation of this return wave in the medium saturated by the strong wave. In such a situation, the return wave is generated by the saturated medium itself and its frequency ω' , which will be dependent on the linear gain and saturation properties of the amplifying medium, will not necessarily be equal to the pump frequency ω . The above formula (61) and similar ones obtained from a higher-order calculation could then be used to study this possibility; in particular, the threshold condition for oscillation at ω' will be obtained by comparing the "linear gain" (64) with the losses of a resonant cavity surrounding the active medium.

*Work part of a research program supported by the Bureau National de Metrologie.

†Permanent address.

¹P. H. Lee and M. L. Skolnick, *Appl. Phys. Letters* **10**, 303 (1967); V. S. Letokhov, *Zh. Eksperim. i Teor. Fiz. Pis'ma v Redaktsiyu* **6**, 597 (1967) [*Sov. Phys. JETP Letters* **6**, 101 (1967)].

²R. G. Brewer, M. J. Kelley, and A. Javan, *Phys. Rev. Letters* **23**, 559 (1969); C. Bordé, *Compt. Rend.* **271**, 371 (1970); T. W. Hänsch, M. D. Levenson, and A. L. Schawlow, *Phys. Rev. Letters* **26**, 946 (1971).

³R. L. Barger and J. L. Hall, *Phys. Rev. Letters* **22**, 4 (1969); N. G. Basov, M. V. Danileiko, and V. V. Nikitin, *Zh. Eksperim. i Teor. Fiz. Pis'ma v Redaktsiyu* **12**, 95 (1970) [*Sov. Phys. JETP Letters* **12**, 66 (1970)].

⁴W. R. Bennet, Jr., *Phys. Rev.* **126**, 580 (1962); *Comments At. Mol. Phys.* **2**, 10 (1970).

⁵V. S. Letokhov, *Comments At. Mol. Phys.* **2**, 181 (1970).

⁶See for example C. Cohen-Tannoudje and J. Dupont-Roc, *Phys. Rev. A* **5**, 968 (1972); and references in E. B. Aleksandrov, A. M. Bunch-Bruevich, N. N. Kostin, and V. A. Khodovoi, *Zh. Eksperim. i Teor. Fiz. Pis'ma v Redaktsiyu* **3**, 85 (1966) [*Sov. Phys. JETP Letters* **3**, 53 (1966)].

⁷S. H. Autler and C. H. Townes, *Phys. Rev.* **100**, 703 (1955).

⁸E. V. Baklanov and V. P. Chebotaev, *Zh. Eksperim. i Teor. Fiz.* **60**, 552 (1971) [*Sov. Phys. JETP* **33**, 300 (1971)].

⁹In fact, the authors were unaware of the work of Baklaev and Chebotaev (Ref. 8) at the time this paper was prepared and only learned of its existence after the present article had been submitted for publication. Accordingly, the introduction of this paper has been modified to acknowledge this substantial work and emphasize the differences between the two papers.

¹⁰W. E. Lamb, Jr., *Phys. Rev.* **134**, 1429 (1964).

¹¹S. Stenholm and W. E. Lamb, Jr., *Phys. Rev.* **181**, 618 (1969).

¹²H. K. Holt, *Phys. Rev. A* **2**, 233 (1970).

¹³B. J. Feldman and M. S. Feld, *Phys. Rev. A* **1**, 1375 (1970).

¹⁴Th. Hänsch and P. Toschek, *Z. Physik* **236**, 213 (1970).

¹⁵N. Bloembergen and Y. R. Shen, *Phys. Rev.* **133**, 37 (1964).

¹⁶Equations (19) are exactly equivalent to the well-

known saturation solution of the Bloch equations. See for example, A. Abragam, *Principes of Nuclear Magnetism* (Oxford U. P., London, 1961).

¹⁷S. Stenholm, *Phys. Rev. B* **1**, 15 (1970).

¹⁸The particular case when all the relaxation rates are equal is the one in which the differences between the hole-burning model and the complete one are the most striking. This point is stressed in Ref. 8, where it is shown that the rate-equations formalism gives good results when $\gamma/\gamma_{ab} \ll 1$ and is inadequate when $\gamma/\gamma_{ab} = 1$. In the present paper, we discuss in detail only this last case.

¹⁹It is clear that the two nonlinear resonant processes considered here are the only ones when the probe field is dealt with to the first order (only one photon of this field can come into play in those processes).

²⁰F. Bloch, *Phys. Rev.* **102**, 104 (1956); W. A. Anderson, *Phys. Rev.* **102**, 151 (1956); F. Hartmann, *IEEE J. Quantum Electron.* **QE5**, 595 (1969).

²¹Level-splitting effects in saturated absorption are also discussed in Ref. 8. Similar effects involving dynamic Stark splitting in a three-level system subjected to laser action have already been studied. See Ref. 14 and references therein.

²²B. Senitzky, G. Gould, and S. Cutler, *Phys. Rev.* **130**, 1460 (1963).

²³J. Gilbert and R. M. Vaillancourt, *Proc. IEEE* **54**, 514 (1966).

²⁴In Ref. 22, the calculations are made in an approximation which amounts to considering the dimensions of the cell to be negligible compared to the wavelength; this is of course not the case in our optical experiment. On the other hand, in the saturated-absorption situation, the pump as well as the probe, is detuned at the same time from the atomic frequency (when $kv \neq 0$), which is not the case in the rf experiment described in Ref. 22. These differences, as well as the fact that the probe field corresponds to a unique sideband instead of two, explain that the amplification effects observed in both situations are only qualitatively comparable. We must in particular notice that the range of pump intensities for which the effect takes place is not the same in both cases: A saturation parameter $I^2 = 3$ is large enough to provide amplification on the sidebands in the rf experiment [see Fig. 7(b)], but is not sufficient to allow the amplification of the weak-return wave in the saturated-absorption experiment (see Fig. 5).

²⁵The problem of amplification of an unique side band by a two-level system driven at resonance by a strong

pump field has in fact been explicitly considered in a recent paper [B. R. Mollow, *Phys. Rev. A* **5**, 2217 (1972)] which deals with stationary atoms irradiated by spatially uniform em fields (long-wavelength approximation). It is in particular shown in this reference that the probe-amplification vs detuning-frequency curve exhibits a small absorption bump zero detuning which is quite similar to the one observed in the probe-amplification vs velocity curves of Fig. 5.

²⁶S. Haroche, *Ann. Phys. (Paris)* **6**, 189 (1971); and C. Cohen-Tannoudji, *Cargese Lectures in Physics*

(Gordon and Breach, New York, 1967).

²⁷A. P. Kol'chenko, S. G. Rautian, and R. I. Sokolovskii, *Zh. Eksperim. i Teor. Fiz.* **55**, 1864 (1968) [*Sov. Phys. JETP* **28**, 986 (1969)].

²⁸P. R. Berman and W. E. Lamb, Jr., *Phys. Rev. A* **2**, 2435 (1970).

²⁹The case of two quasiresonant waves propagating in the same direction in a gaseous medium is considered in a recent paper: E. V. Baklanov and V. P. Chebotaev, *Zh. Eksperim. i Teor. Fiz.* **61**, 922 (1971) [*Sov. Phys. JETP* **34**, 490 (1972)].

PHYSICAL REVIEW A

VOLUME 6, NUMBER 4

OCTOBER 1972

Double-Photon Transitions in Microwave Spectroscopy

F. Chiarini, M. Martinelli and S. Santucci

Istituto di Fisica della Università-Pisa, Italy

and Gruppo Nazionale di Struttura della Materia-Consiglio Nazionale delle Ricerche-Pisa, Italy

and

P. Bucci

Istituto di Chimica della Università-Napoli, Italy

and Gruppo Nazionale di Struttura della Materia-Consiglio Nazionale delle Ricerche-Napoli, Italy

(Received 21 March 1972)

The expression for the absorption coefficient in two-photon resonance transitions is deduced under general conditions. No particular restrictions are imposed on the level system or on the frequencies and intensities of the fields. The following cases are considered: (i) a two-level system (with and without singularities) irradiated by a single wave and (ii) a three-level system irradiated by two waves. Some theoretical and experimental disagreements reported by authors of previous papers are examined and clarified by the present theory.

I. INTRODUCTION

Oka and Shimizu¹ have recently shown the possibility of some experiments of a new kind concerning double-photon electric dipole transitions in the microwave frequency region. These experiments were carried out on a system of three rotational levels, E_0 , E_1 , E_2 .

The variation of the resonance signal relative to the $E_0 \rightarrow E_1$ transition was detected using a second strong pumping wave.

The frequency of the pumping wave satisfied the conditions

$$\omega_p \simeq (E_2 - E_1)/2\hbar \quad (\text{degenerate case})$$

or

$$\omega_p \simeq (E_2 - E_0)/2\hbar \quad (\text{nondegenerate case}).$$

Finally Oka and Shimizu compared their experimental results with theoretical predictions deduced from the semiclassical Karplus-Schwinger theory.²

However some disagreements can be found: (i) To fit the experimental data to the theoretical pre-

dictions, a relaxation time quite different from that obtained from the pressure-broadening parameter must be assumed. (ii) Experimental results on the PF_3 molecule (low dipole moment) are not in agreement with the theory. (iii) Field attenuation within the Stark cell is neglected.

Mollow³ discussed a similar case of resonant two-photon absorption from a theoretical point of view. Considering a pair of levels in two-photon resonance and using a semiclassical approach, he calculated the time evolution of the density matrix and the shift produced by radiation. These results, obtained by irradiation with a single wave, were analogous to those reported in Ref. 1.

In particular Mollow found that the radiation-induced shift increases and becomes large when an intermediate-state energy approaches the mean of energies corresponding to active states of the system. The mathematical expression for the shift shows singularities when the wave frequency is single-photon resonant between one of the actual levels and a third one of the system. Of course, this happens because the conditions are not ful-